UNITED STATES DEPARTMENT OF THE INTERIOR

GEOLOGICAL SURVEY

Report on Direct Current Soundings
Over a Geothermal Prospect in the
Bruneau-Grand View Area, Idaho

By

Dallas B. Jackson

Open-file report 74-240

1974

Contents

Illustrations

/¯Plates are in pocket_/

Report on Direct Current Soundings Over a

Geothermal Prospect in the Bruneau-Grand View Area, Idaho

---

by Dallas B. Jackson

The U.S. Geological Survey has completed two electrical resistivity

studies in the southwest part of Idaho, between the towns of Oreana and

Hammett (pl. 1). The purpose of these studies was to investigate an

area identified as a potential geothermal area by Young and Mitchell

(1973). The first survey, an audio-magnetotelluric (AMT) survey, com-

pleted in the early summer of 1973 (D. B. Hoover, written commun., 1974),

defined a conductivity anomaly extending from near the town of Oreana on

the west to within about 10 km of Hammett on the east. The conductive

region, as outlined by the AMT survey for apparent resistivities measured

at 8 Hz, is shown on plate 1. I have chosen to discuss the 8-Hz AMT map

because 8 Hz was the lowest frequency recorded and thus represents the

greatest depth of penetration measured in the AMT survey. The 8-Hz con-

tours clearly show a major low-resistivity area at the west end of the

map area, bounded by steep gradients to the west, south, and northeast,

but extending to the east in a trough-like shape for at least 65 km. The

major departure from this general trend is a sublateral extention of the

conductive zone into the Bruneau Valley, which is interpreted by Hoover

as a narrow fracture zone along which hot waters are rising.

This paper describes the results of the second electrical survey,

made during September 1973; this survey consisted of 31 d-c soundings

used to verify the AMT anomalies and to define the vertical extent of the conductive body. The soundings were arranged along 2 profiles: 1) a profile approximately east-west along the axis of the AMT anomaly, crossing the steep AMT resistivity gradient at the west end and extending about 85 km, to beyond the end of the AMT anomaly to the east; the exposed rocks along this profile are primarily alluvial and lake deposits of middle to late Pleistocene age, although some basalt flows of middle Pleistocene age were also traversed along the east-central part of the profile north of Bruneau (Malde and others, 1963, Young and Mitchell, 1973); 2) a profile south-southeast from the center of the closed 5 ohm-m AMT contour to the steep resistivity gradient 17 km to the south; the exposed rocks beneath this profile range from lower Pleistocene alluvial and lake deposits at the north end to basalt flows and silicic volcanic rocks of Pliocene age at the south end. In addition to the soundings along the profiles, two soundings were made north of the AMT anomaly about halfway between Bruneau and Mountain Home.

Geophysical technique and interpretation

All the vertical electrical soundings were made with the Schlumberger array using direct current (Keller and Frischknecht, 1966). The apparent resistivities, $\bar{\rho}_s$, were calculated from the equation:

$$\bar{\rho}_s = \frac{(\overline{AB}/2)^2 - (\overline{MN}/2)^2}{\overline{MN}} \cdot \frac{\Delta V_{mn}}{I}$$

where $\overline{AB}$ and $\overline{MN}$ are the current and potential electrode spacings, V_{mn} is the potential difference between the M and N electrodes, and I is the input current. $\bar{\rho}_s$ then is expressed in ohm-m^2/m or more commonly,

2

simply as ohm-m. By convention, the results are plotted on bilogarithmic paper with apparent resistivity plotted in the Y direction and the spacing $\overline{AB}/2$ plotted in either feet or metres in the X direction.

All the VES curves except 1 and 30, which were badly distorted, were interpreted after smoothing of lateral effects and correcting for bad jumps (Kunetz, 1956) using an automatic interpretation program developed by A. A. R. Zohdy (written commun., 1974). The detailed solutions from the automatic interpretation program were simplified by smoothing of Dar Zarrouk curves calculated for the detailed layering, to provide better correlation between adjacent soundings (Zohdy, 1974a). Theoretical curves were then computed for the assumed layer thickness and resistivities (Zohdy, 1974b) and compared to the field curves. An example of field data, the computed theoretical curve, and the layered resistivity model plotted at the bottom of the graph paper for VES 15 are shown in figure 1.

Sounding interpretations

Thirty-one soundings were completed in the Bruneau-Grand View area with $\overline{AB}/2$ spacings ranging from 900 to 3700 m. The field curves for these soundings, neither smoothed nor adjusted for jumps or lateral effects, are shown in figures 2-32. All of the sounding interpretations except for VES 1, 30, and 31 are shown on profiles A-A' and B-B' (pl. 2).

Layer resistivities calculated from the sounding curves have been grouped into five semilogarithmic ranges to simplify the correlation of electrical layers from sounding to sounding. Where two clearly defined layers fall within a resistivity range, such as at VES 11 (profile A-A'),

3

both layer resistivities are noted, 3.2 and 6.5 ohm-m, and the layer boundary is marked by a dashed line. In addition, where layers from adjacent soundings appear to correlate, but one of the layers has a resistivity that places it just within a higher or lower resistivity range, such as the fourth layer from the surface at VES 6 (profile A-A'), the layer resistivity is noted by parentheses, for example (17.4), and the resistivity-range pattern for the layer from the adjacent sounding (the 18-36 ohm-m range from the 21 ohm-m beneath VES 22) is carried through.

Profile A-A', which lies along the axis of the AMT low, is underlain at the surface for most of its length by alluvial and lacustrine deposits of Quaternary age. The rapid lateral variations of these sedimentary layers in the upper 300 to 600 m are clearly shown by the poor correlation of electrical units from sounding to sounding. Resistivity variations within this part of the section are compatible with resistivities that have been observed in other areas for similar lithologies, ranging from as much as several hundred ohm-m for dry or well-washed gravels to less than 10 ohm-m for clay or clay-rich sands (Zohdy and others, 1969; Keller and Frischknecht, 1966).

Of more interest than the near-surface electrical units is the conductive unit, which ranges in resistivity from 2.8 ohm-m beneath VES 23 to 7 ohm-m beneath VES 8, and varies in thickness from about 360 m beneath soundings 8, 22, and 25 to about 900 m beneath soundings 10, 15, and 24. Presumably, this is the unit which causes the resistivity low on the 8-Hz AMT map. Six wells along profile A-A' penetrate the

4

conductive 1-7 ohm-m unit and each well extends through the sediments
of the Idaho Group at least into the Banbury Basalt; all but 2 of the
wells (well 13ada1 and well 16bbb1) bottom in Idavada silicic volcanics.
No electrical contrasts exist between the Idaho Group and Banbury Basalt
or between the Banbury Basalt and Idavada Volcanics.

Although fresh basalts near the surface usually have resistivities
of the order of 100 ohm-m or greater, their resistivity decreases with
burial beneath the water table and as the amounts of alteration products
increase. Resistivity values for the unweathered basalts of the Bruneau
Formation in the survey area were measured beneath soundings 3, 2, 28,
and 23, and range from about 77 ohm-m at VES 3 to about 295 ohm-m at
VES 2. Resistivity values approaching 500 ohm-m were measured for the
near-surface basalts of the Snake River Group and the Bruneau Formation
beneath VES 31 (fig. 33). Resistivities for weathered Hawaiian basalts
buried beneath the water table have been reported by Zohdy and Jackson
(1969) to be as low as 30 ohm-m; Keller and Rapolla (in press) report
resistivities as low as 10-20 ohm-m for sequences of freshwater saturated
basalts in other parts of the world. Increased temperature, salinity,
and alteration products will further decrease the formation resistivity.
Dissolved solids in water analysis of the Bruneau-Grand View-area water
wells are generally well below 1000 mgm/l (Young and Mitchell, 1973),
which suggests that the low resistivity of the Banbury Basalt and
Idavada Volcanics in the 1-7 ohm-m unit is probably due to a combination
of high-temperature water and increased amounts of alteration products
that would tend to form in a hydrothermal environment.

The source of the thermal fluids is unresolved but it seems likely that they rise along basement faults, many of which are interpreted to be present along profile A-A' and are transmitted laterally in the permeable layers. One such source is suggested by the AMT low that extends southeastward into the mouth of Bruneau Canyon. The trend of this low coincides with the rapid thickening of the 1-7 ohm-m layer beneath VES 23 and 24. Also lying along this trend is a residual magnetic high whose source is relatively shallow, about 1 km (D. R. Mabey, oral commun., 1974). The magnetic high could be caused by hypogene enrichment of magnetite above the postulated fault zone. The major portion of the magnetic high lies south of the sounding profile, although a nose of the anomaly does extend beneath VES 23. The thick layer of 7-18 ohm-m material underlying the 1-7 ohm-m layer may also contain thermal waters, but this thick layer has a lower porosity than the Idavada Volcanics higher in the section and thus has a higher resistivity. If the contact between the high-resistivity basement layer and the base of the 7-18 ohm-m layer coincides with the base of the Idavada Volcanics, then thicknesses of Idavada Volcanics greater than 1,200 m are implied in the vicinity of VES 13-VES 16 and VES 2-VES 26.

Although the 8-Hz AMT anomaly appears to die out to the east, electrical soundings show that it extends eastward at least as far as VES 27, where the 1-7 ohm-m layer is about 640 m thick. The failure of the AMT soundings to detect the continuation of the lower resistivity zone to the east may mean that the zone is restricted laterally and that the 8-Hz AMT resistivities reflect a combination of higher resistivity material to the north and south, in addition to the more conductive material beneath the AMT sounding stations.

Electrical basement rises to the west between VES 9 and VES 10, coincident with the steep 8-Hz AMT gradient on plate 1, and the resistivities of both the 1-7 and 7-18 ohm-m layers begin to increase west of VES 10, thus suggesting a permeability barrier in that direction.

Profile B-B', extending south from the west end of the AMT low, clearly shows the thinning of the low-resistivity layers and the up-faulting of the electrical basement to the south. Between VES 19 and VES 18 the 1-7 ohm-m layer nearly disappears and the thin section of 1-7 ohm-m material beneath VES 18, about 45 m thick, probably represents a layer of clay-rich lacustrine deposits of the upper Pliocene Glenns Ferry Formation. The existence of these faults is also clearly shown by the offset on the basalt in wells 10bdd1 and 21cbc1 on the profile. Hot water is present in well 21cbc1 and may originate in the 28 ohm-m layer beneath VES 18 that thins rapidly to the south. A steep gradient on the 8-Hz AMT map also occurs between VES 18 and VES 19, reflecting the loss of the low-resistivity horizons mentioned above; however, a bowing of the 100 ohm-m 8-Hz contour to the south from VES 18 may indicate that the low-resistivity horizons extend to the southeast, perhaps beneath a greater thickness of overburden or simply with increasing resistivities.

Two soundings, VES 30 and VES 31, were made north of the main AMT anomaly (pl. 1), on the basalt plateau north of Bruneau, to see if any trace of the low-resistivity units could be detected where the increased overburden thickness might screen them from the AMT soundings. Both VES 30 (fig. 31) and VES 31 (figs. 32, 33) clearly show the presence of a conductor at AB/2 spacings greater than 300 m. Sounding 30 is too distorted by lateral effects to model effectively, but VES 31, although its rising terminal branch is not developed, suggests a layer of about 3 ohm-m about 250 m thick, followed by a more resistive layer of perhaps 20 ohm-m. This interpretation suggests that the 1-7 ohm-m layer is thinner at VES 31 than at any other sounding location, perhaps suggesting that the zone of hot water is pinching out to the north.

Conclusions

The d-c sounding survey confirms the presence of a large conductive section of sedimentary and volcanic rocks underlying the low-resistivity AMT anomaly defined by Hoover. Within the conductive section, resistivity boundaries between sedimentary rocks of the Idaho Group, the Banbury Basalt, and Idavada Volcanics appear to be entirely obscured, at least where well data are available. True resistivities near these contacts range from about 3-5.5 ohm-m, about 3 to 10 times less than would be expected for similar volcanic rock types saturated with fresh water. Because water samples from wells in the Bruneau-Grand View area are relatively fresh, the greatly decreased resistivities are probably related to a combination of thermal waters and alteration within the volcanic rocks and perhaps also within part of the sedimentary section.

8

The d-c soundings trace the low resistivity zone beyond the limits of the AMT survey to the east as far as the town of Hammett, where a zone of 4.4 ohm-m material 640 m thick is present. To the west the conductive section terminates about 5 km east of Oreana, where truncation of the conductive section appears to be related to decreasing lateral porosity. The 1-7 ohm-m conductive section can still be recognized beneath the Snake River Plain between Bruneau and Mountain Home, although the top of the conductor is deeper and the thickness is less than at any other sounding location.

No zones were recognized on any of the soundings where a high-resistivity basement was not detected, with the possible exception of the 21 ohm-m basement layer beneath VES 25, which may be caused by the rapidly thickening sections of low-resistivity material to the east and to the west along the line of sounding expansion. The presence of a high-resistivity basement suggests that thermal fluids probably emanate from greater depths than this survey can resolve, rise along fault zones, of which there appear to be many, and then spread laterally through lithologic units that have sufficient porosity.

References

Keller, G. V., and Frischknecht, F. C., 1966, Electrical methods in geophysical prospecting: New York, Pergamon Press, 519 p.

Keller, G. V., and Rapolla, Antonio, in press, Geoelectrical surveys of thermal areas, in Gasparini, A., Civetta, G., Luongo, G., and Rapolla, A., eds., Physical volcanology: New York, Elsevier Press.

Kunetz, G., 1966, Principles of direct current resistivity prospecting: Berlin-Nikolassee, Gebruder Borntraeger, 103 p.

Malde, H. E., Powers, H. A., and Marshall, C. H., 1963, Reconnaissance geologic map of west-central Snake River Plain, Idaho: U.S. Geol. Survey Misc. Geol. Inv. Map I-373, scale 1:125,000.

Young, H. W., and Mitchell, J. C., 1973, Geochemistry and geologic setting of selected thermal waters, pt. 1 of Geothermal investigations in Idaho: Idaho Dept. of Water Adm., Water Info. Bull. no. 30, 43 p., 2 pl.

Zohdy, A. A. R., 1974a, Use of Dar Zarrouk curves in the interpretation of vertical electrical sounding data: U.S. Geol. Survey Bull. 1313-D, (in press).

_____, 1974b, A computer program for the calculation of Schlumberger sounding curves by convolution: U.S. Geol. Survey Rept. USGS-GD-74-010, 12 p.; available only from U.S. Dept. Commerce Natl. Tech. Inf. Service, Springfield, Va. 22151 as Rept. PB 232 056.

Zohdy, A. A. R., Jackson, D. B., Mattick, R. E., and Peterson, D. L., 1969, Geophysical surveys for ground water at White Sands Missile Range, New Mexico: U.S. Geol. Survey open-file rept. 31 p.

Zohdy, A. A. R., and Jackson, D. B., 1969, Application of deep electrical soundings for ground-water exploration in Hawaii: Geophysics, v. 34, p. 584-600.
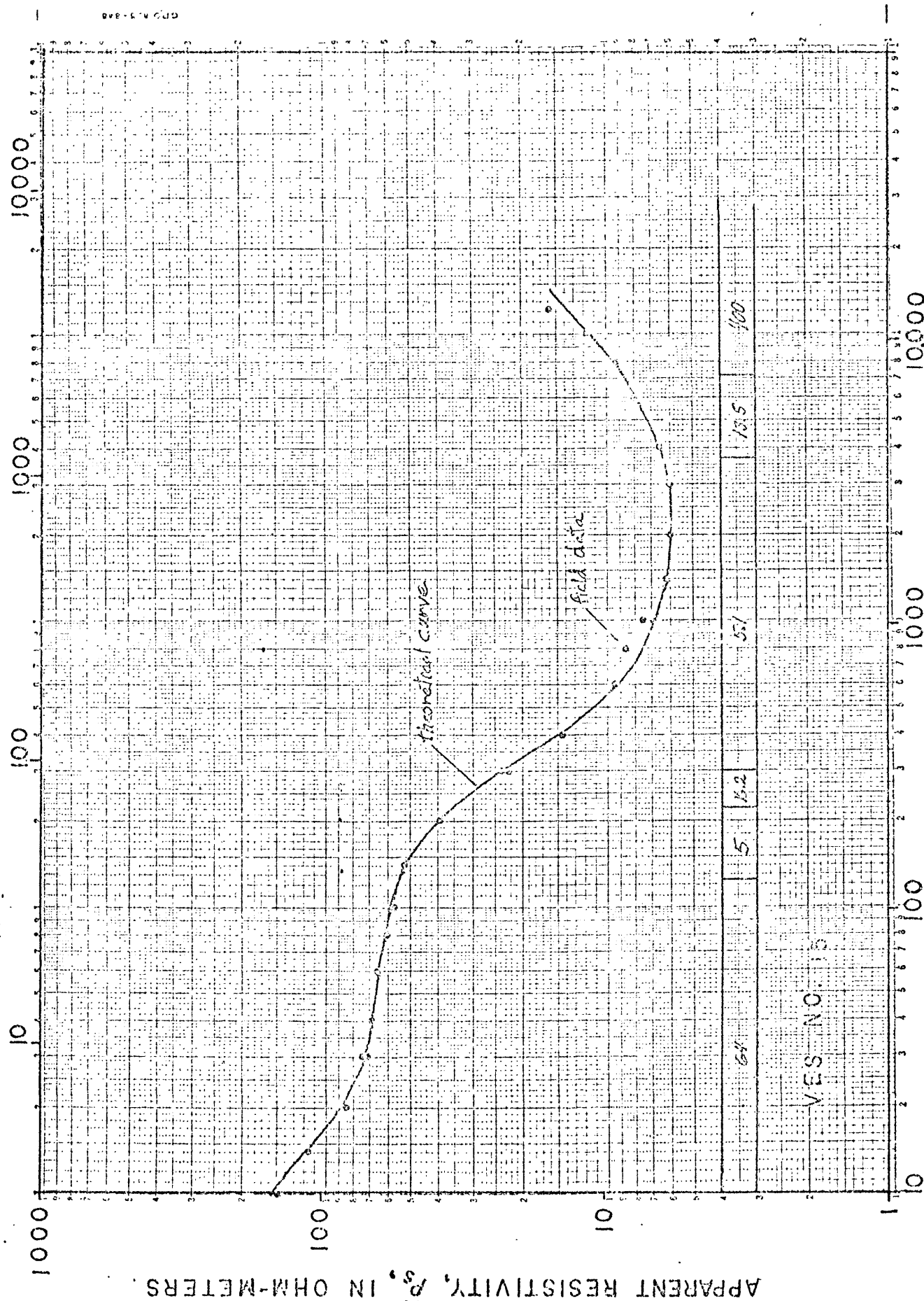
Figure 1.--Example of Schlumberger sounding data (for VES 15) showing a layered resistivity model and a computed theoretical apparent resistivity curve.

ELECTRODE SPACING, AB/2, IN METERS

ELECTRODE SPACING, AB/2, IN FEET

APPARENT RESISTIVITY, $\bar{P}_s$, IN OHM-METERS

VES NO. 1
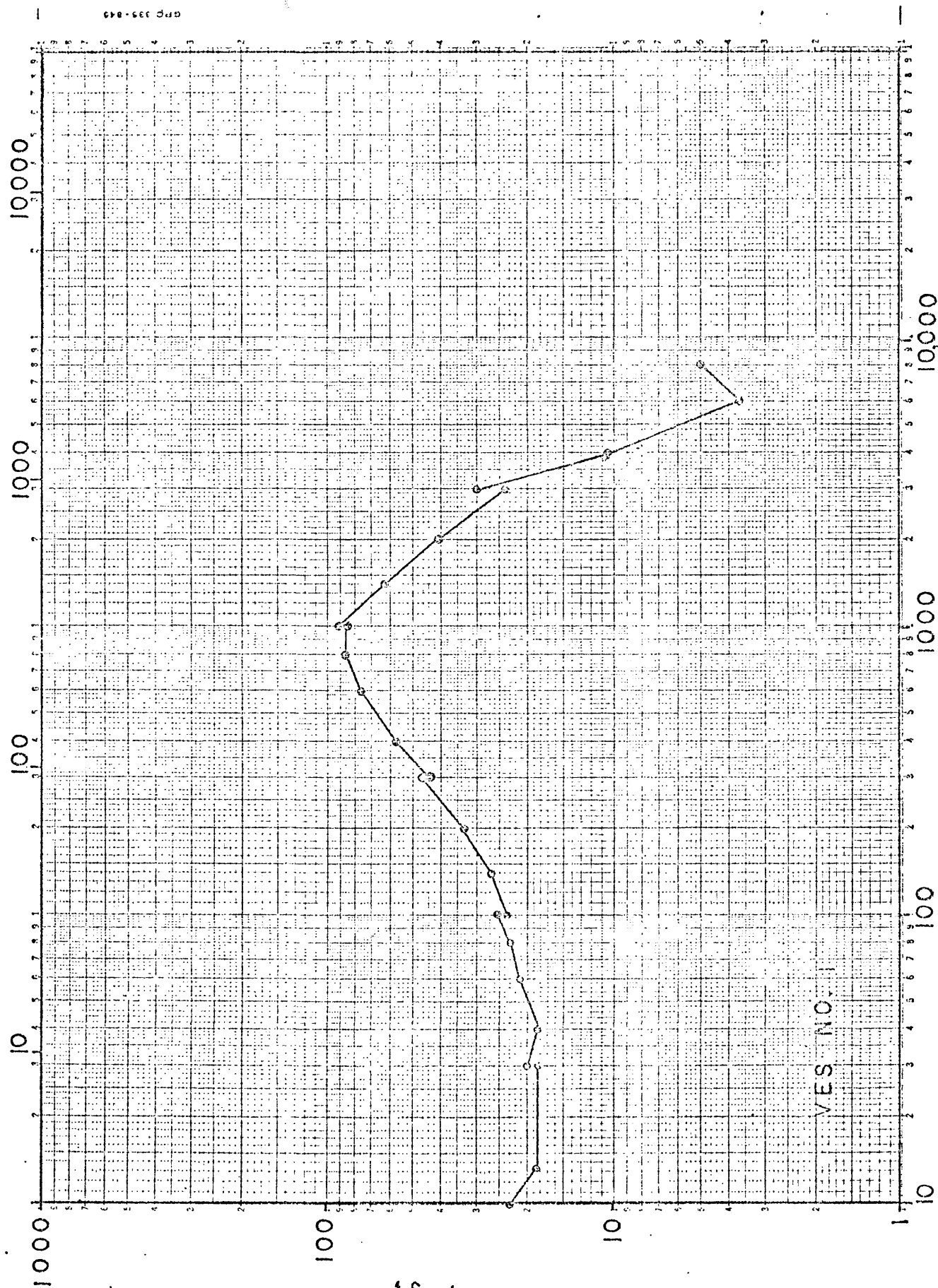
Figure 2.--Schlumberger sounding curve VES 1

ELECTRODE SPACING, AB/2, IN METERS

ELECTRODE SPACING, AB/2, IN FEET

APPARENT RESISTIVITY, $\underline{\rho}_s$, IN OHM-METERS

VES NO. 2
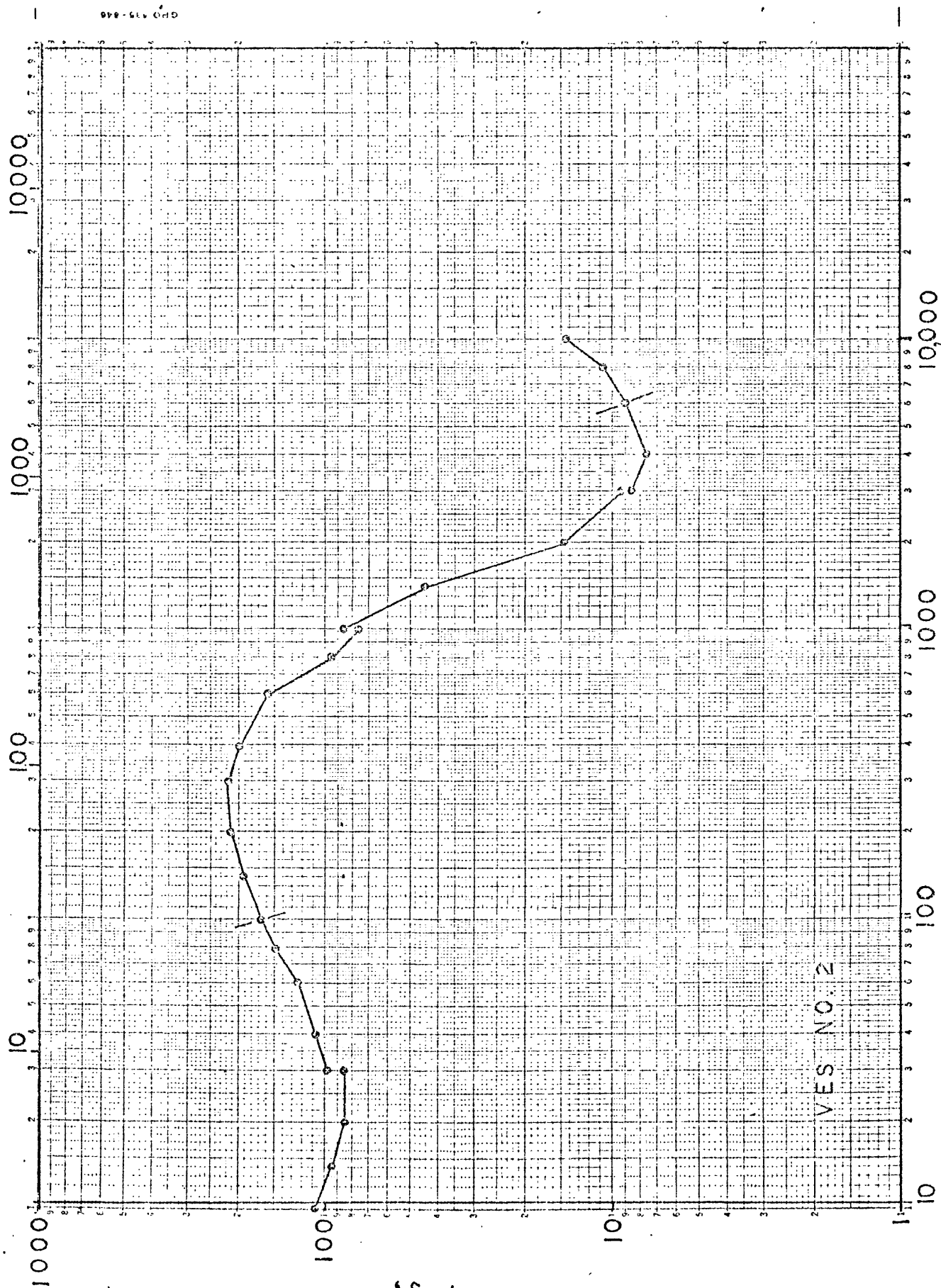
Figure 3.--Schlumberger curve VES 2

14
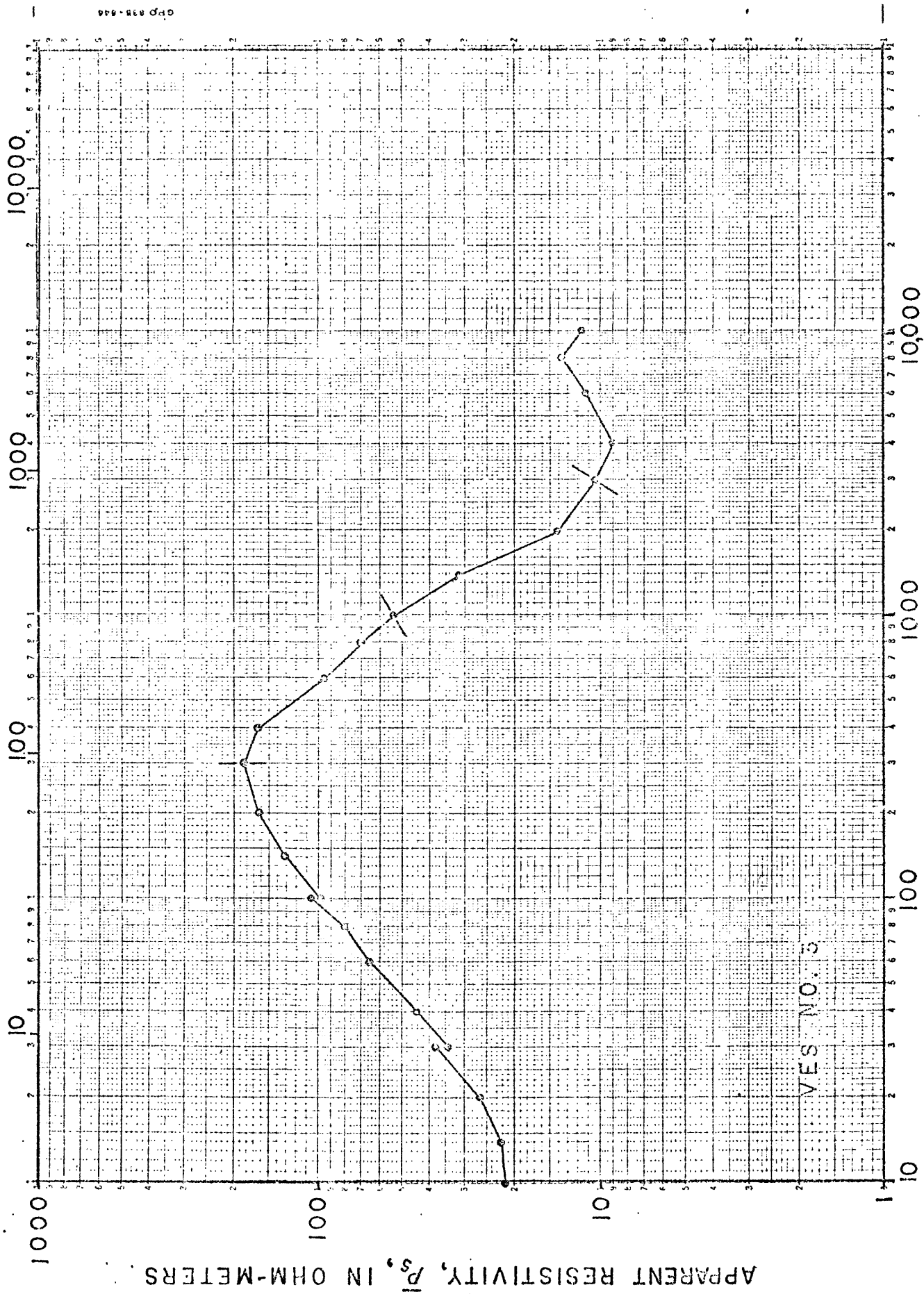
Figure 4.--Schlumberger curve VES 3

ELECTRODE SPACING, AB/2, IN METERS
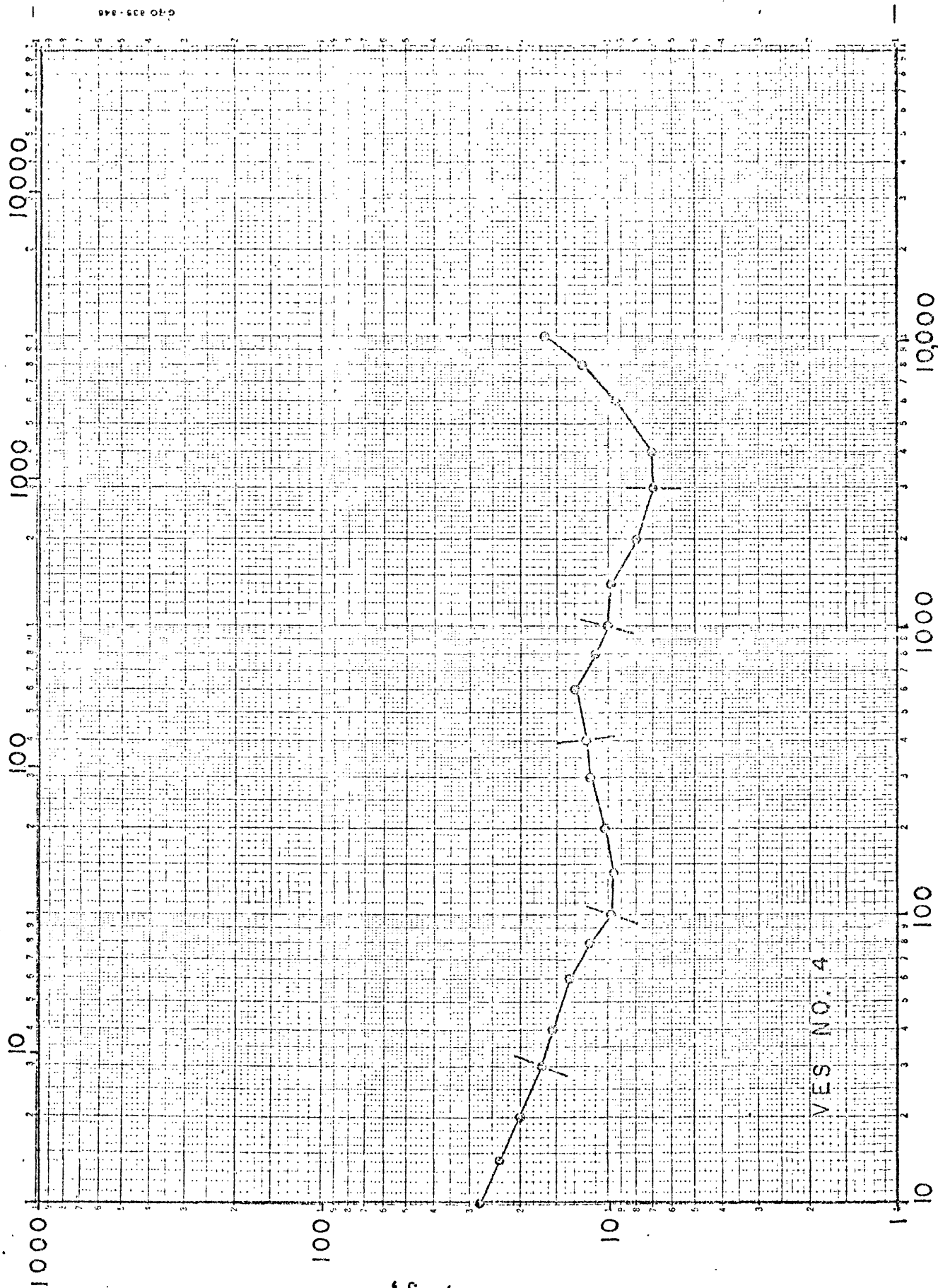
ELECTRODE SPACING, AB/2, IN FEET
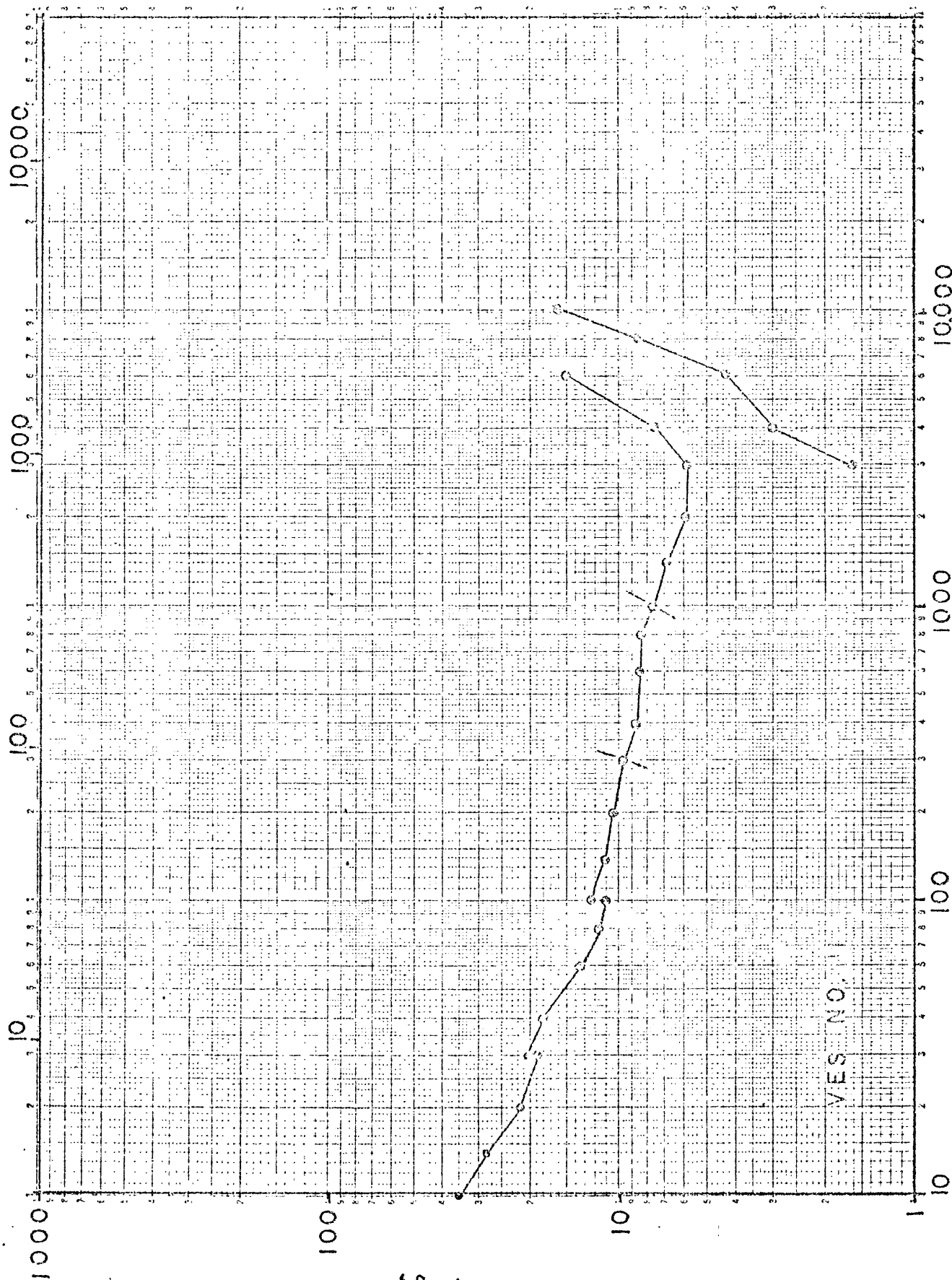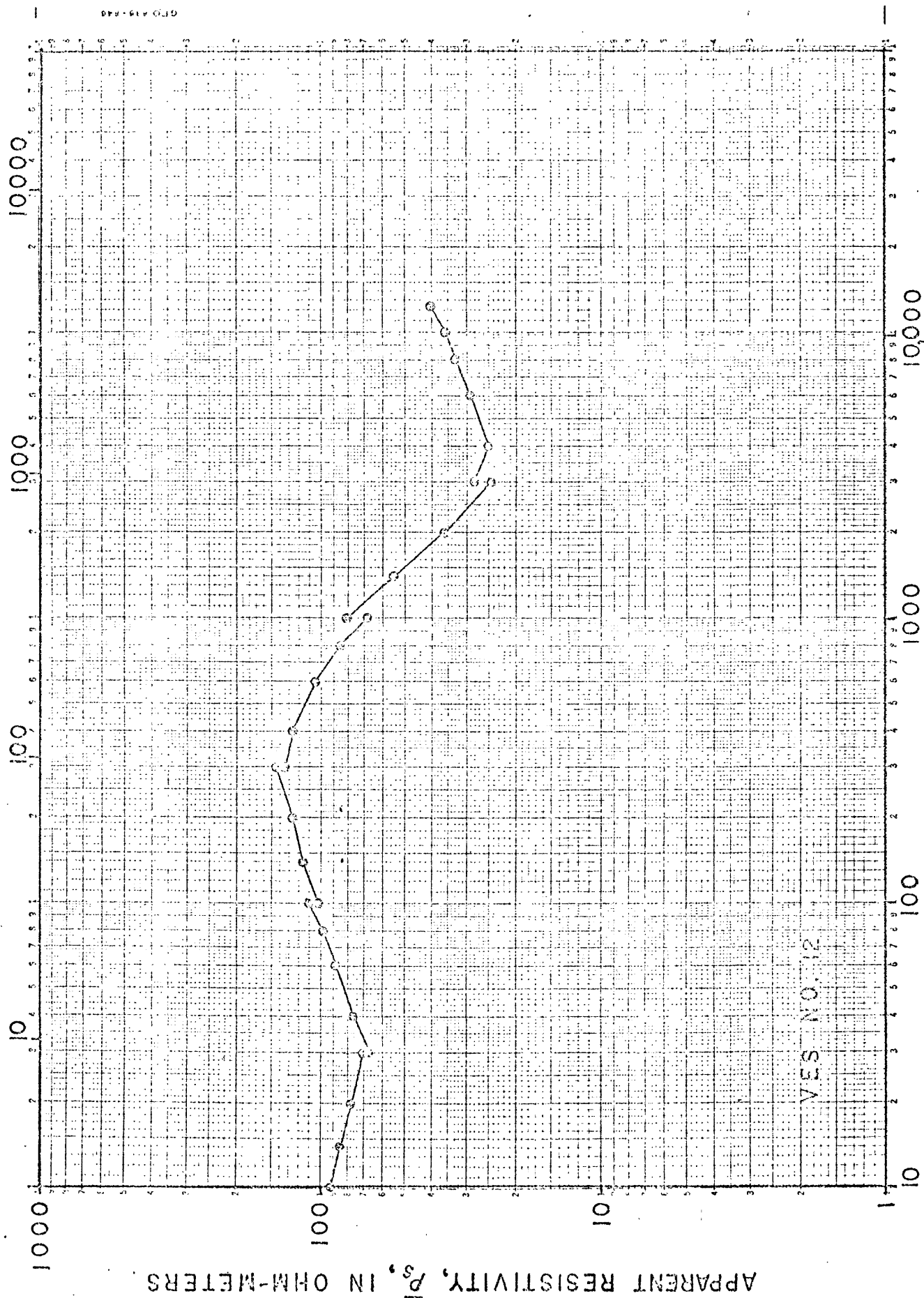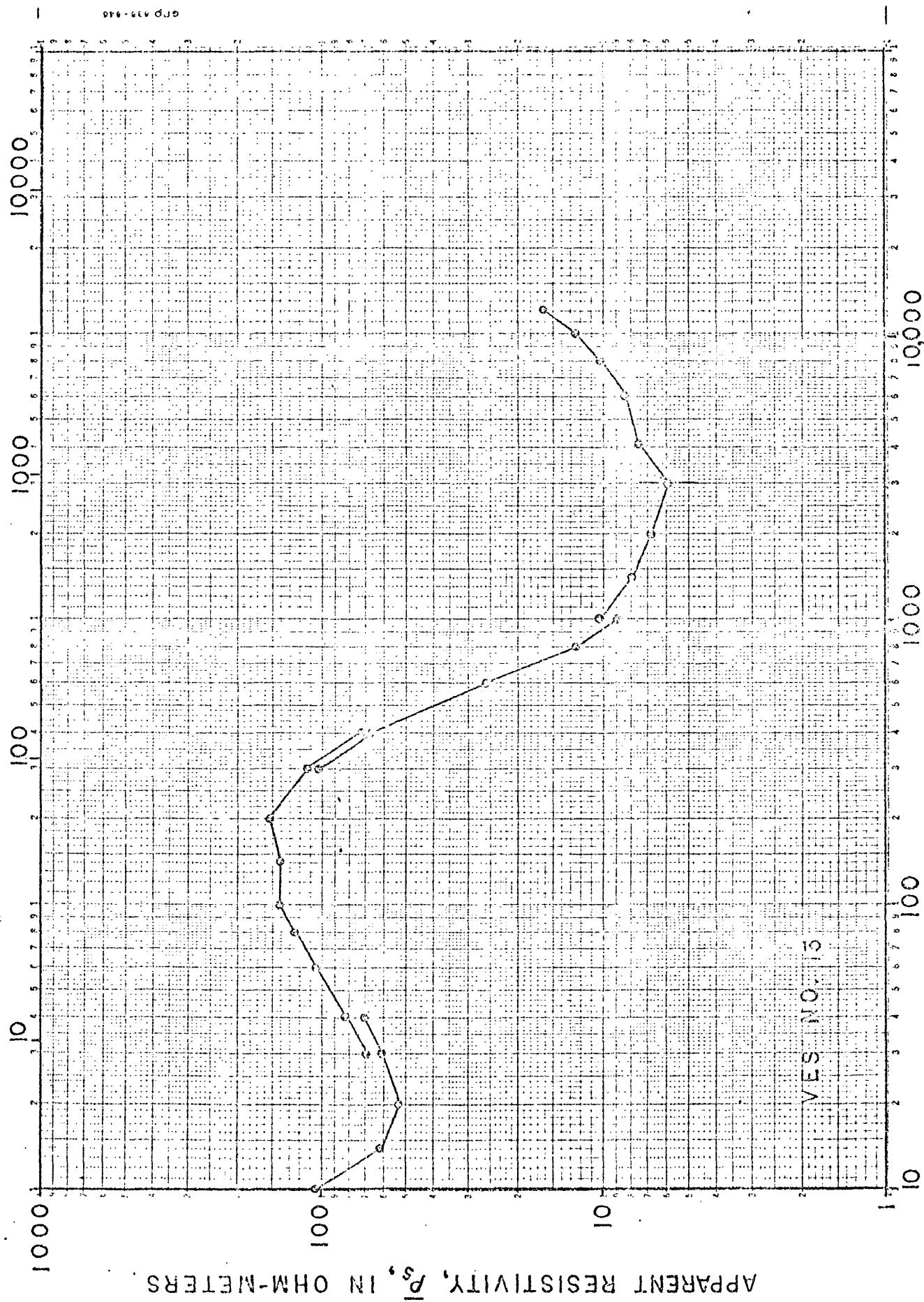
Figure 5.--Schlumberger curve VES 4

VES NO. 4

APPARENT RESISTIVITY, $\overline{\rho}_s$, IN OHM-METERS

ELECTRODE SPACING, AB/2, IN METERS

ELECTRODE SPACING, AB/2, IN FEET
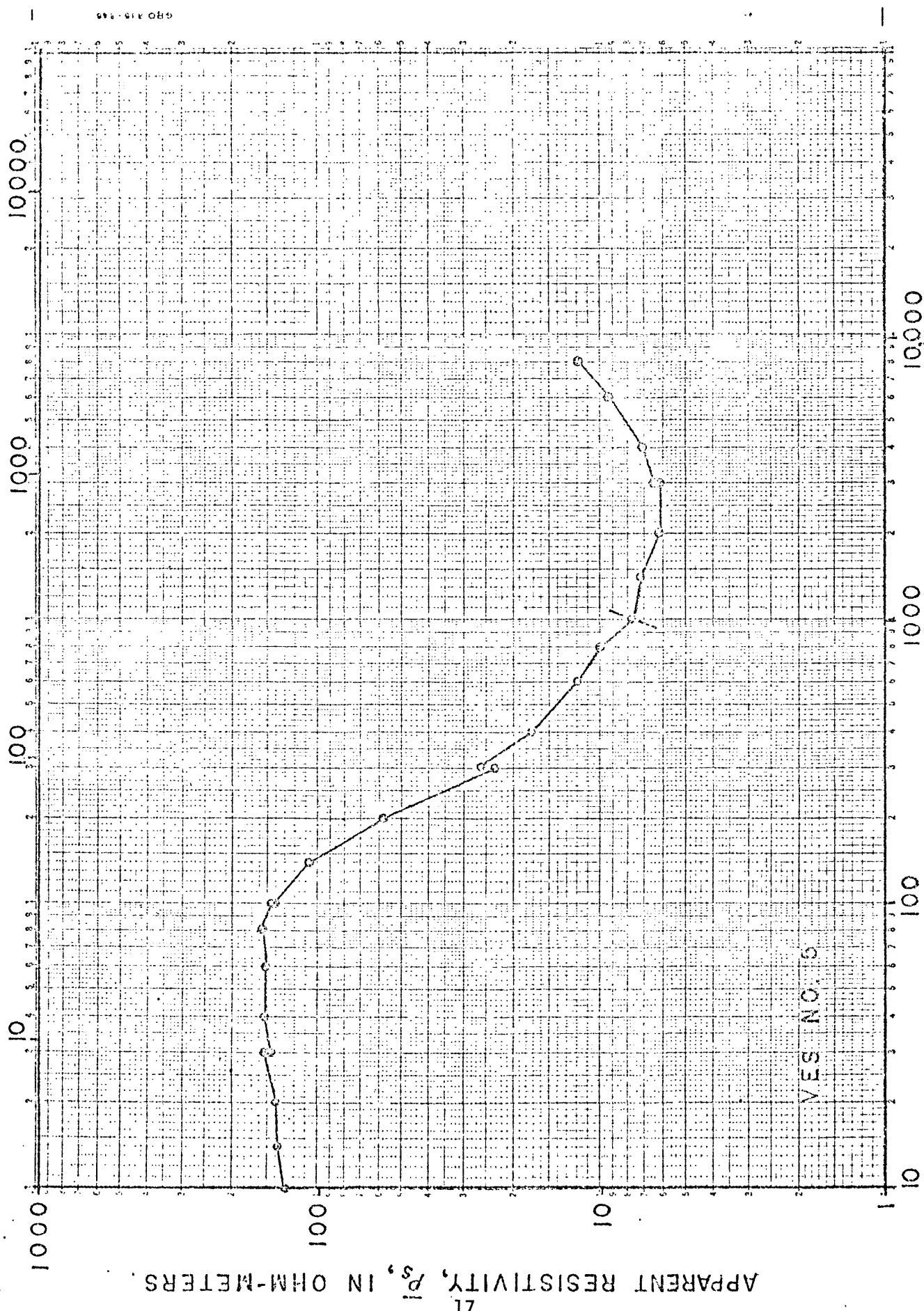
Figure 6.--Schlumberger curve VES 5

APPARENT RESISTIVITY, $\bar{\rho}_s$, IN OHM-METERS

VES NO. 5
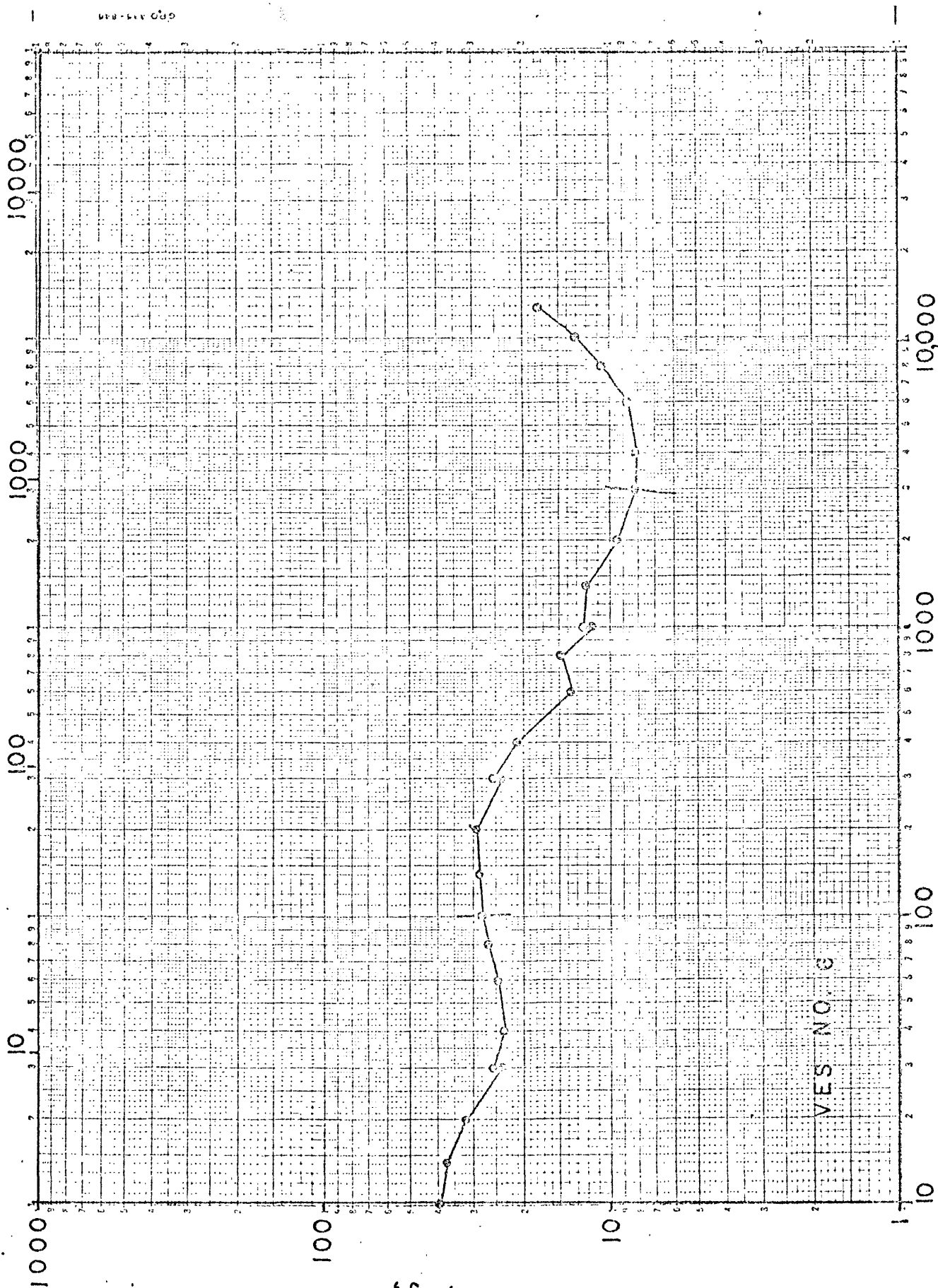
Figure 7.—Schlumberger curve VES 6.

ELECTRODE SPACING, AB/2, IN METERS

ELECTRODE SPACING, AB/2, IN FEET

APPARENT RESISTIVITY, $\bar{P}_s$, IN OHM-METERS

V.E.S. NO. 7
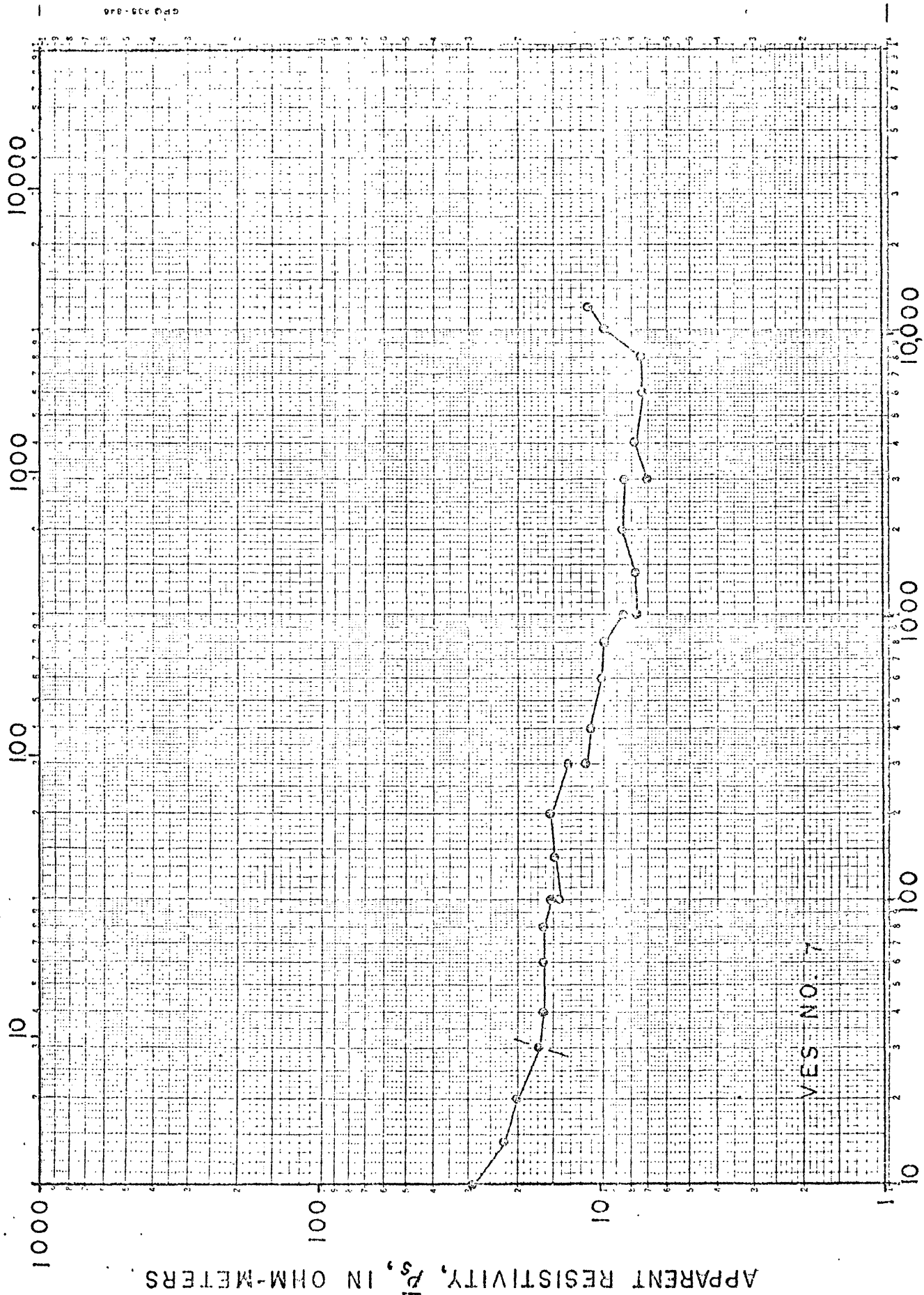
Figure 8.--Schlumberger curve VES 7

ELECTRODE SPACING, AB/2, IN METERS
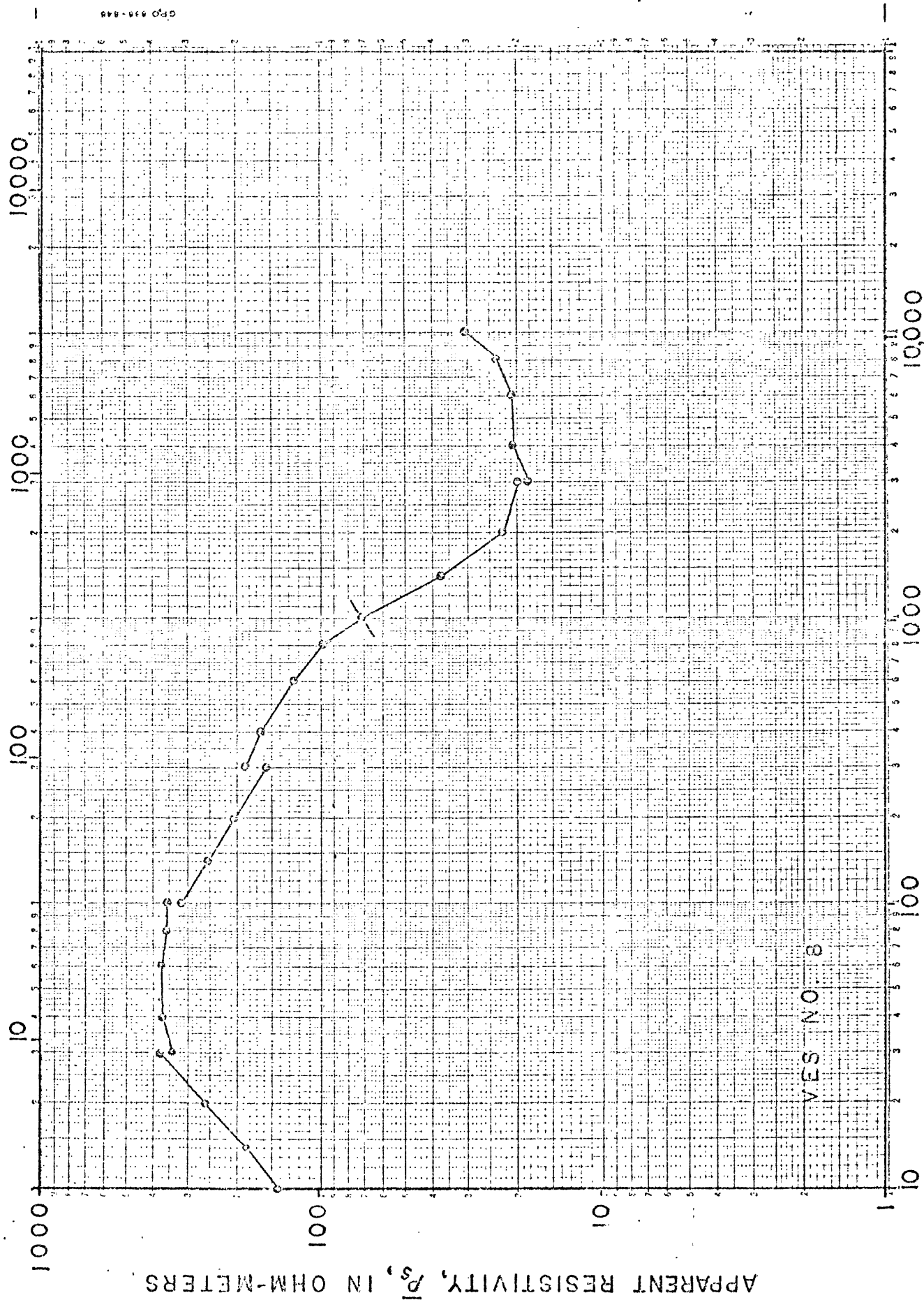
ELECTRODE SPACING, AB/2, IN FEET
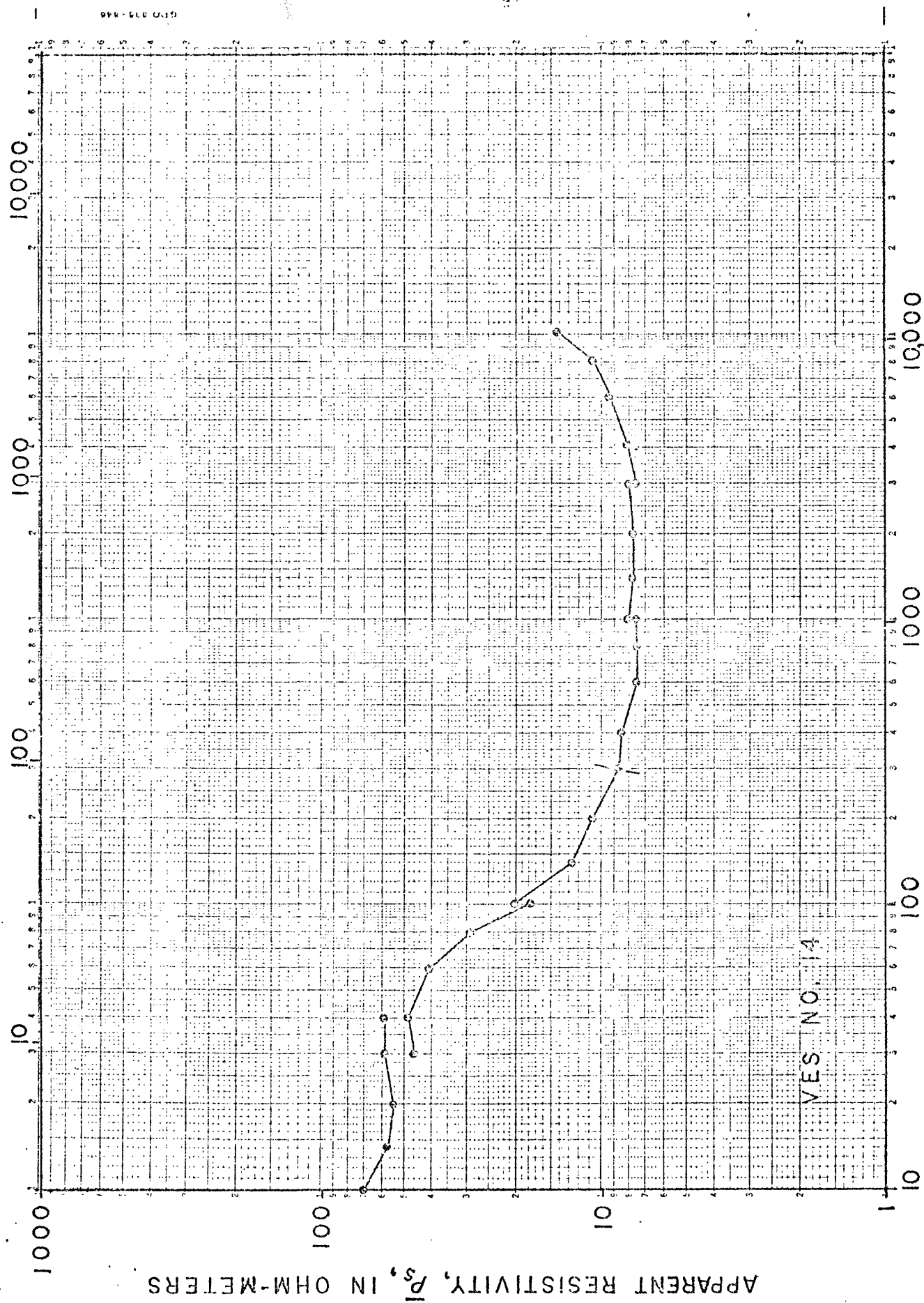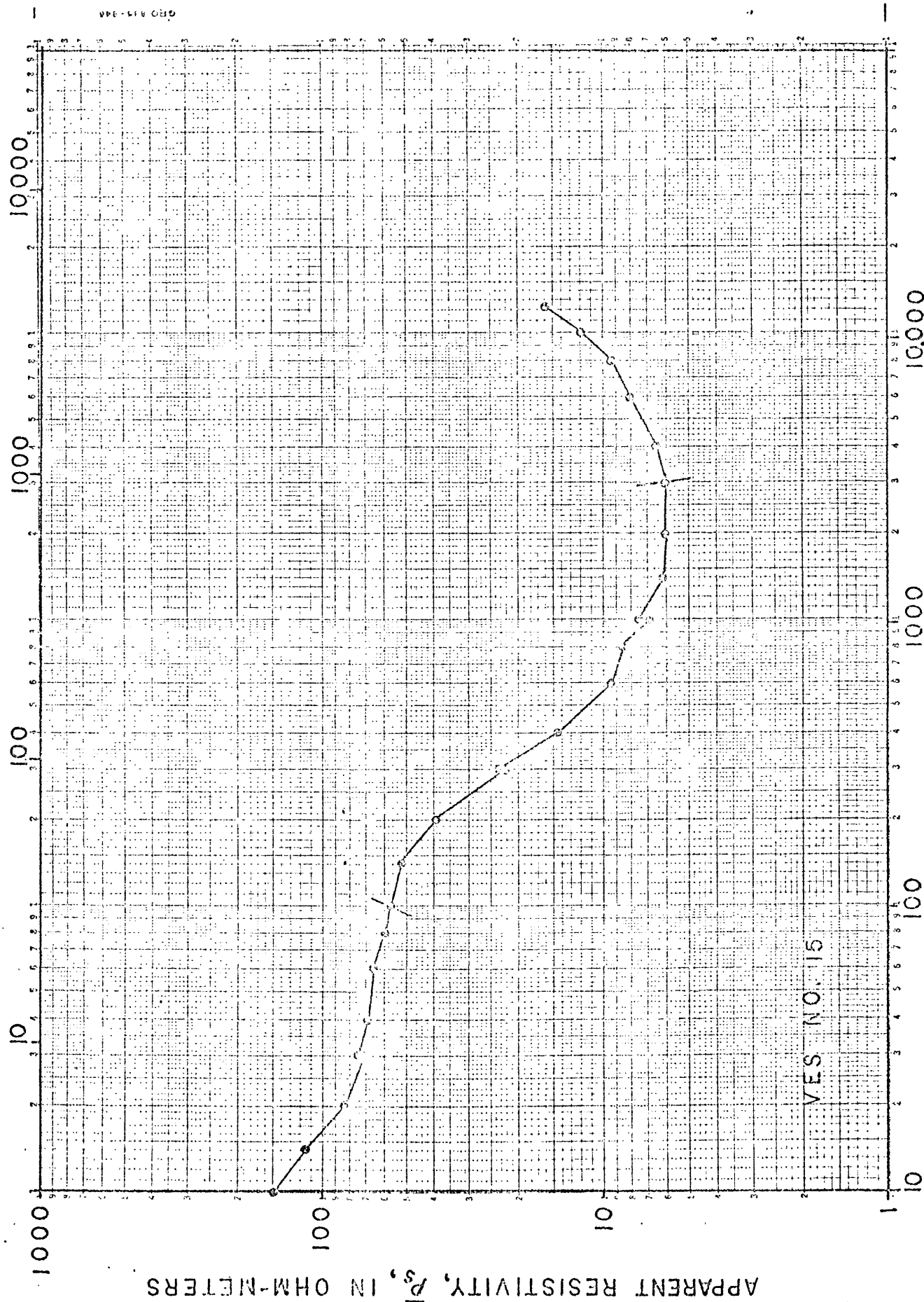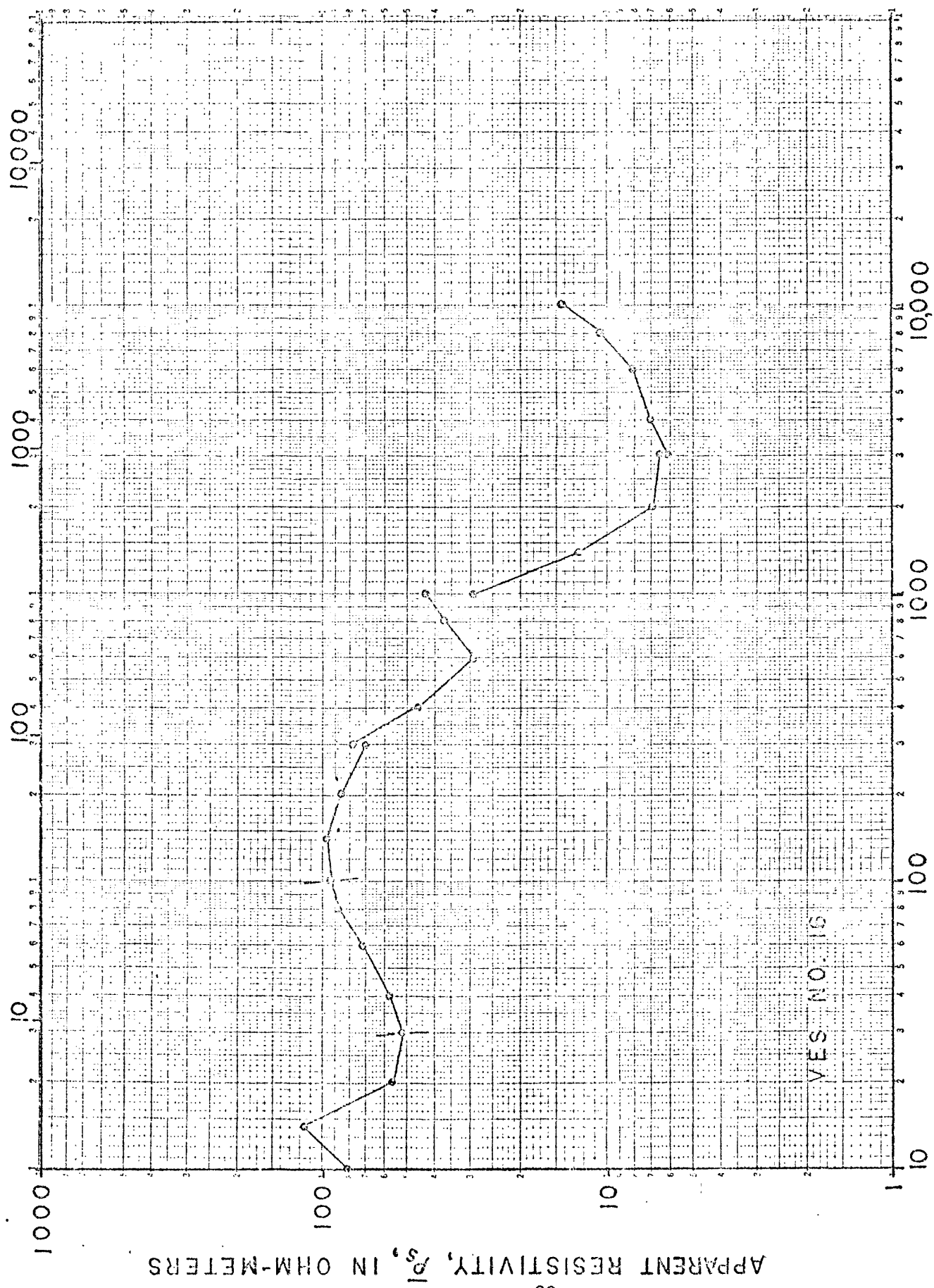
Figure 9.--Schlumberger curve VES 8

VES NO. 8

APPARENT RESISTIVITY, $\bar{P}_s$, IN OHM-METERS

20

ELECTRODE SPACING, AB/2, IN METERS

APPARENT RESISTIVITY, $\bar{P}_s$, IN OHM-METERS

VES NO. 9
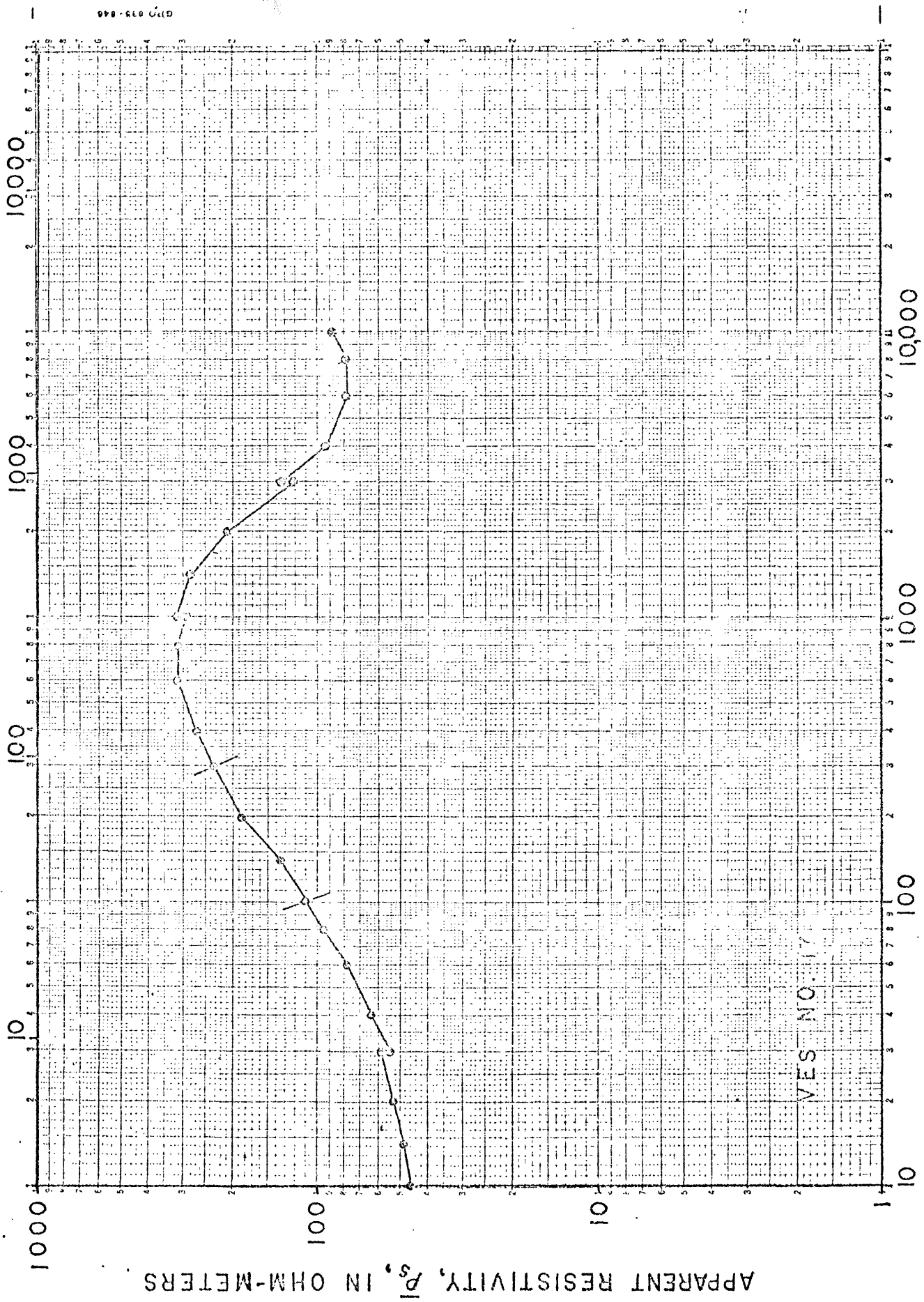
ELECTRODE SPACING, AB/2, IN FEET
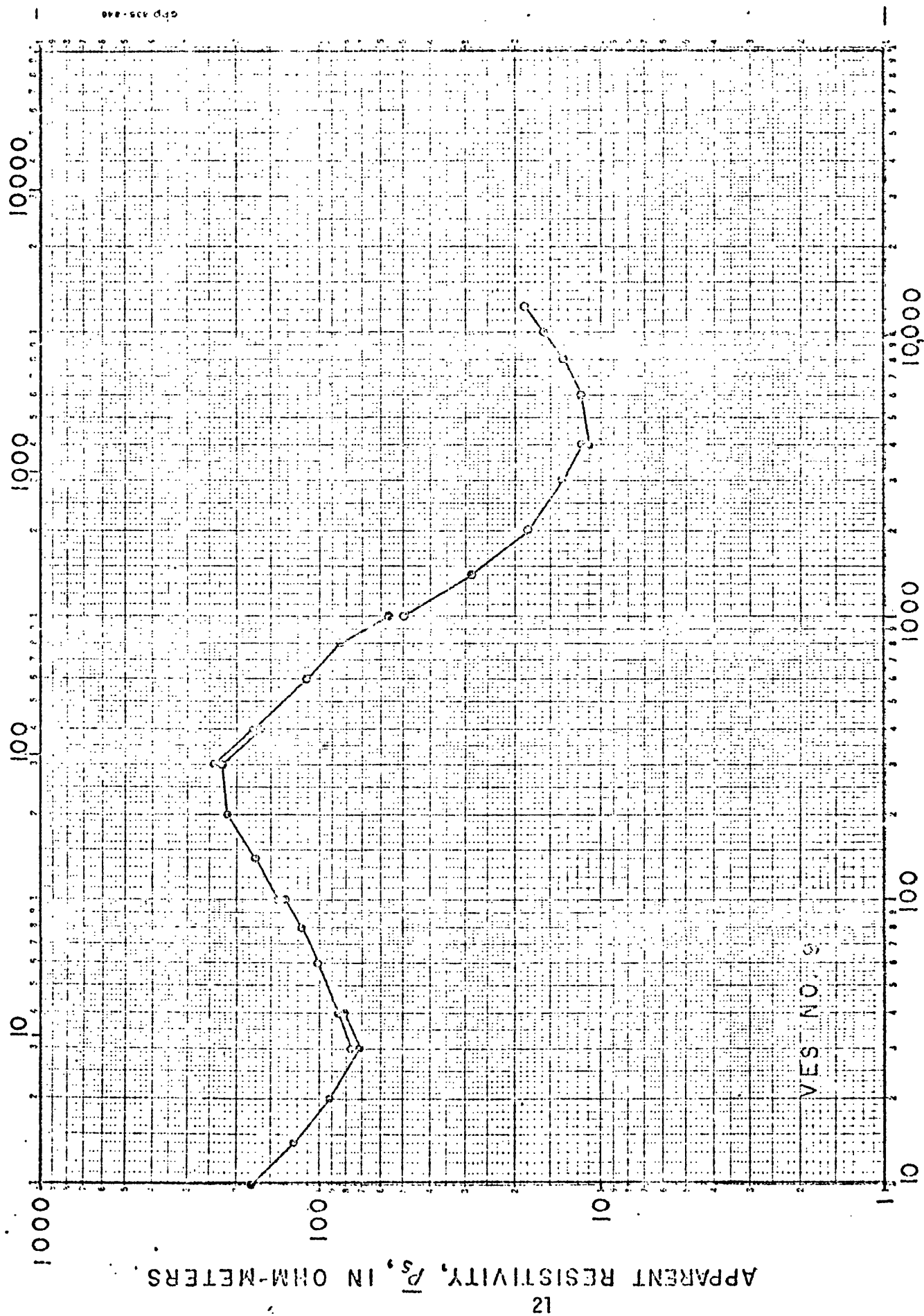
Figure 10.--Schlumberger curve VES 9

ELECTRODE SPACING, AB/2, IN METERS

ELECTRODE SPACING, AB/2, IN FEET

APPARENT RESISTIVITY, $\bar{\rho}_s$, IN OHM-METERS

V.E.S. NO. 10
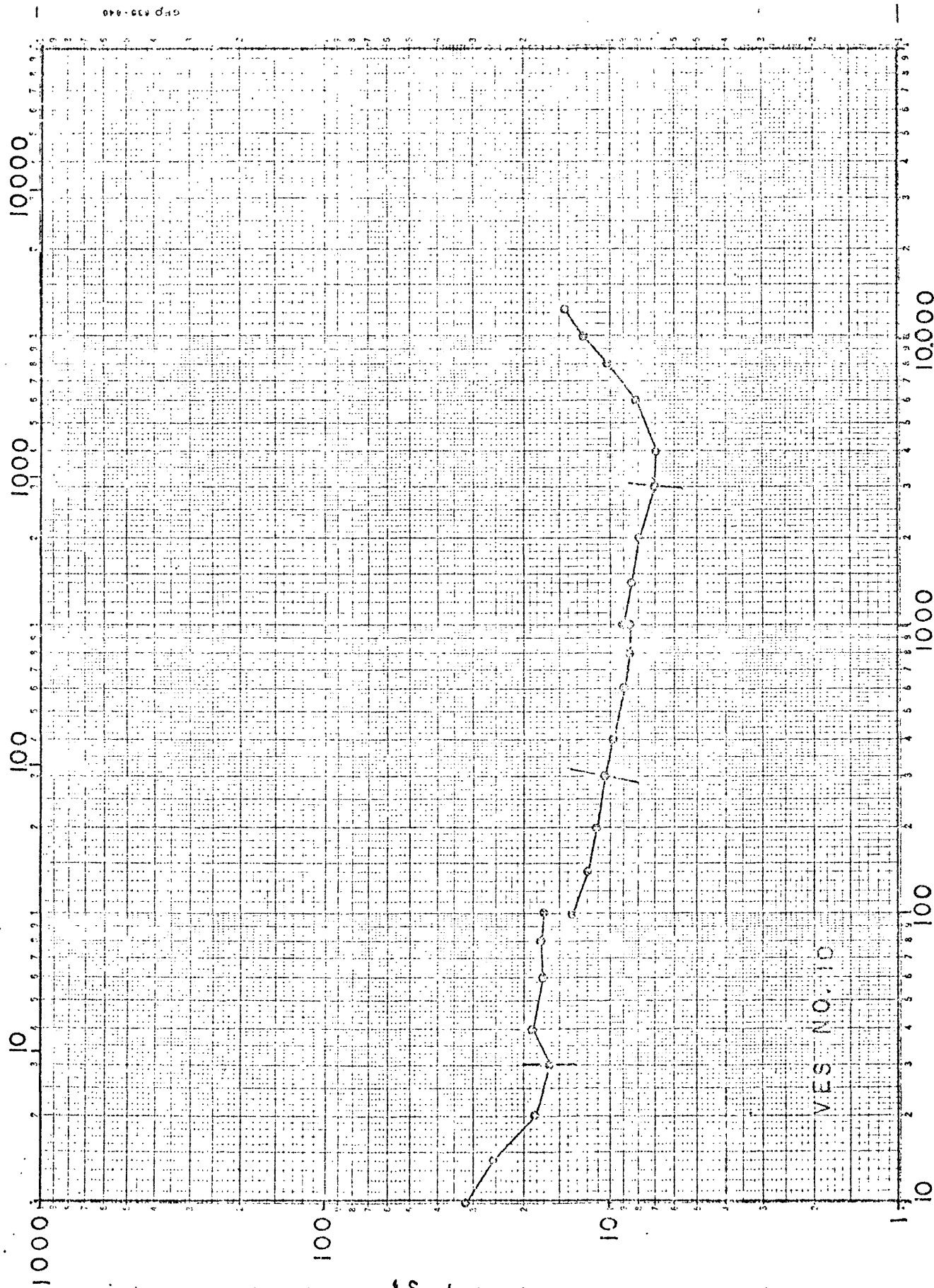
Figure 11.--Schlumberger curve VES 10

ELECTRODE SPACING, AB/2, IN METERS

APPARENT RESISTIVITY, $\bar{P}_s$, IN OHM-METERS

ELECTRODE SPACING, AB/2, IN FEET

VES NO. 11

Figure 12.--Schlumberger curve, VES 11

ELECTRODE SPACING, AB/2, IN METERS

ELECTRODE SPACING, AB/2, IN FEET

Figure 13.--Schlumberger curve VES 12

APPARENT RESISTIVITY, $\bar{P}_s$, IN OHM-METERS

VES NO. 12

ELECTRODE SPACING, AB/2, IN FEET

Figure 14.--Schlumberger curve VES 13

25

ELECTRODE SPACING, AB/2, IN METERS

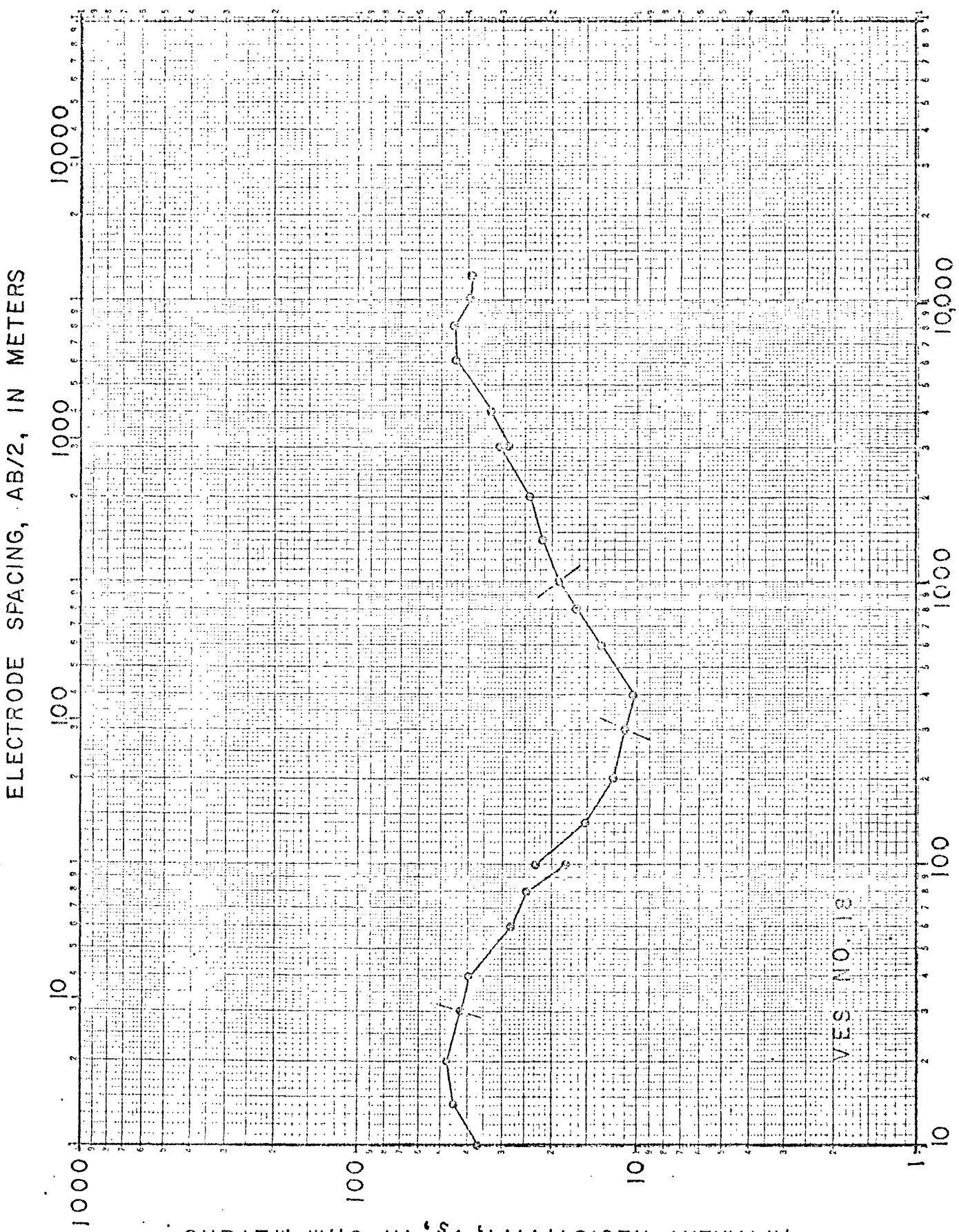ELECTRODE SPACING, AB/2, IN FEET

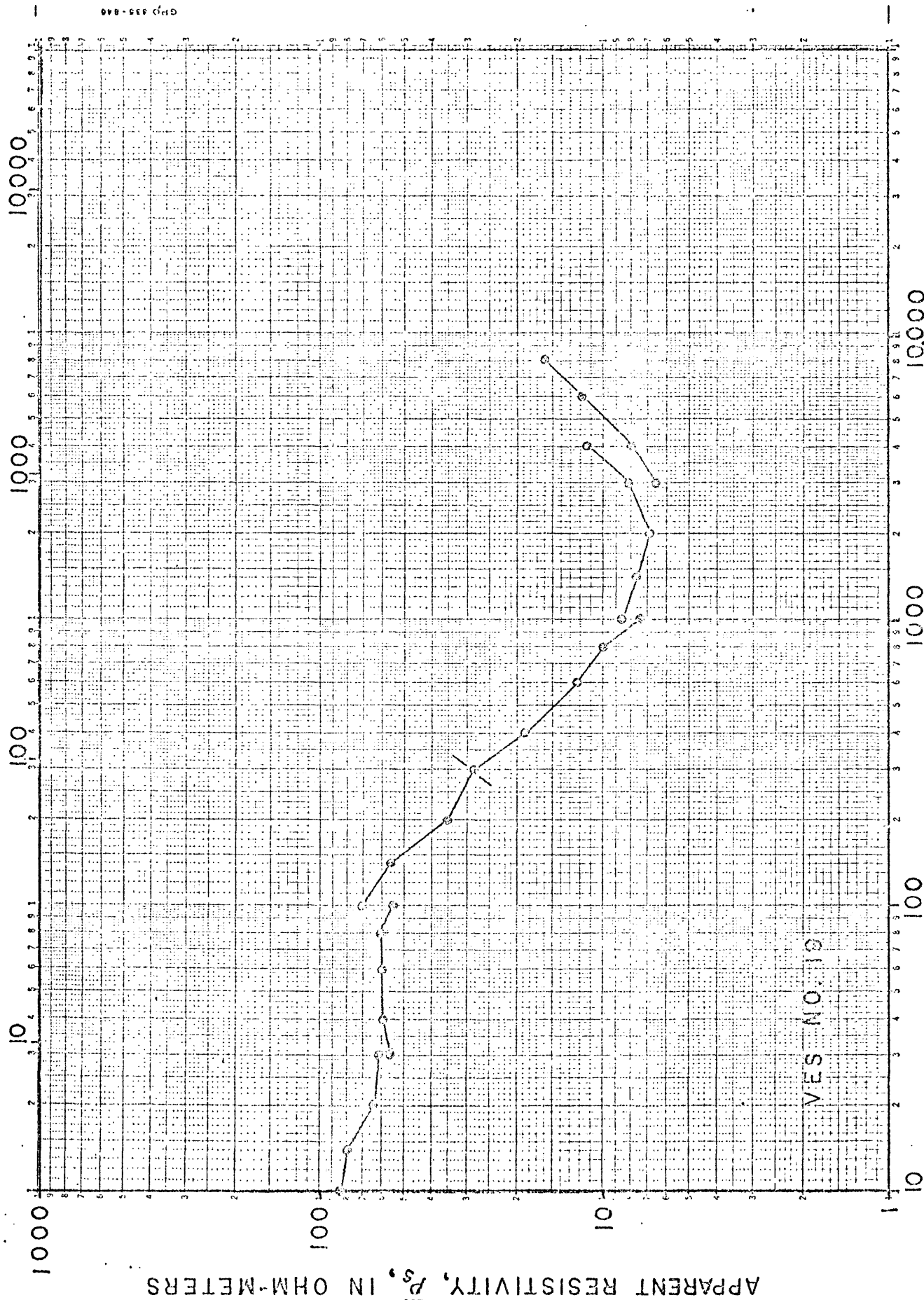Figure 15.--Schlumberger curve VES 14

APPARENT RESISTIVITY, $\underline{P}_s$, IN OHM-METERS

VES NO. 14

26

ELECTRODE SPACING, AB/2, IN METERS

ELECTRODE SPACING, AB/2, IN FEET

APPARENT RESISTIVITY, $\bar{\rho}_s$, IN OHM-METERS

VES NO. 15

Figure 16.--Schlumberger curve VES 15

27

ELECTRODE SPACING, AB/2, IN METERS

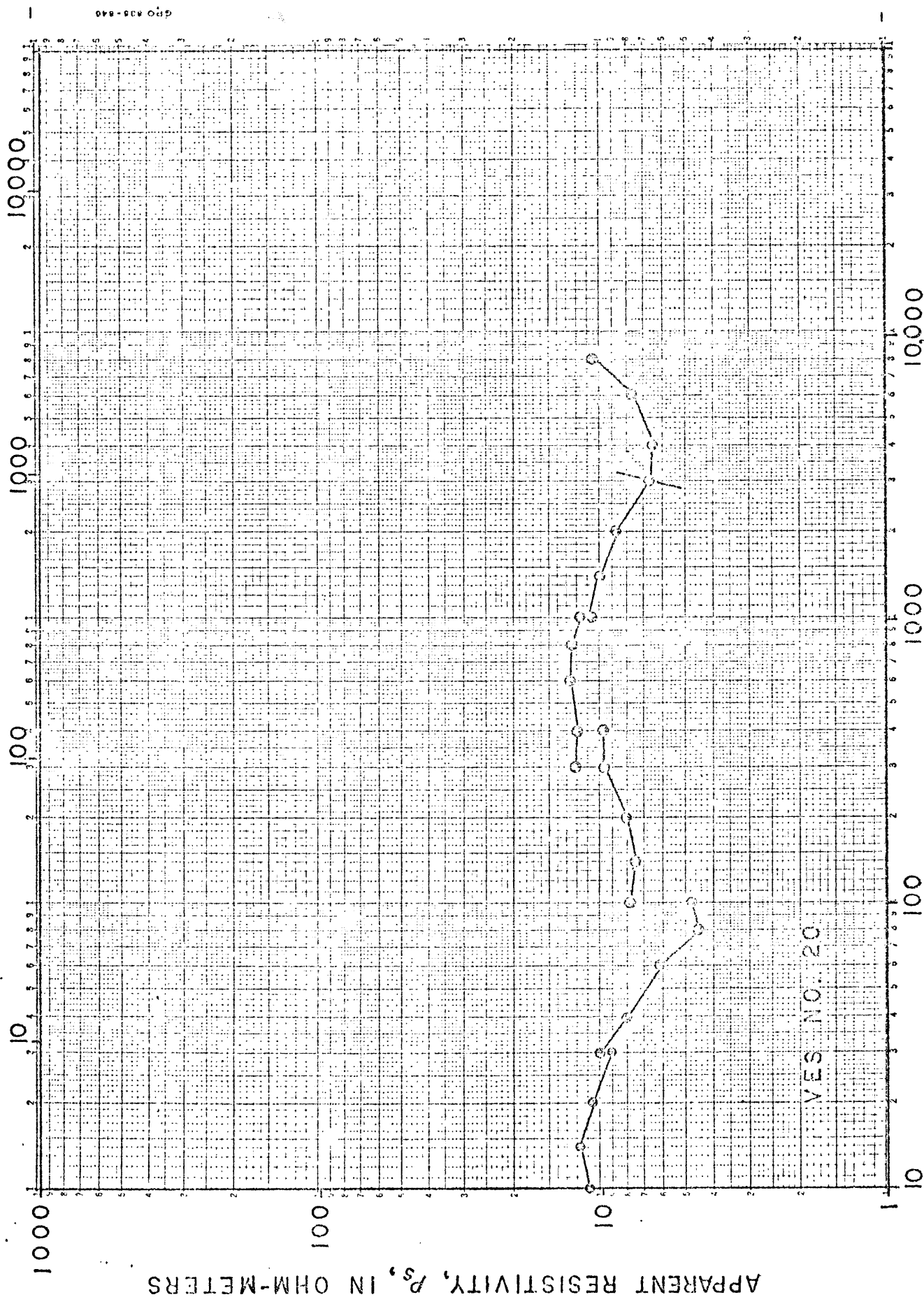ELECTRODE SPACING, AB/2, IN FEET

Figure 17.--Schlumberger curve VES 16

APPARENT RESISTIVITY, $\underline{\rho}_s$, IN OHM-METERS

VES. NO. 16

ELECTRODE SPACING, AB/2, IN METERS

ELECTRODE SPACING, AB/2, IN FEET

Figure 18.--Schlumberger curve VES 17

VES NO. 17

APPARENT RESISTIVITY, $\bar{P}_s$, IN OHM-METERS

29

ELECTRODE SPACING, AB/2, IN METERS

ELECTRODE SPACING, AB/2, IN FEET

Figure 19.--Schlumberger curve VES 18

VES NO. 18

APPARENT RESISTIVITY, $\overline{P}_s$, IN OHM-METERS

30

ELECTRODE SPACING, AB/2, IN METERS

ELECTRODE SPACING, AB/2, IN FEET

Figure 20.--Schlumberger curve VES 19

APPARENT RESISTIVITY, $\bar{P}_s$, IN OHM-METERS

31

ELECTRODE SPACING, AB/2, IN METERS

APPARENT RESISTIVITY, $\bar{\rho}_s$, IN OHM-METERS

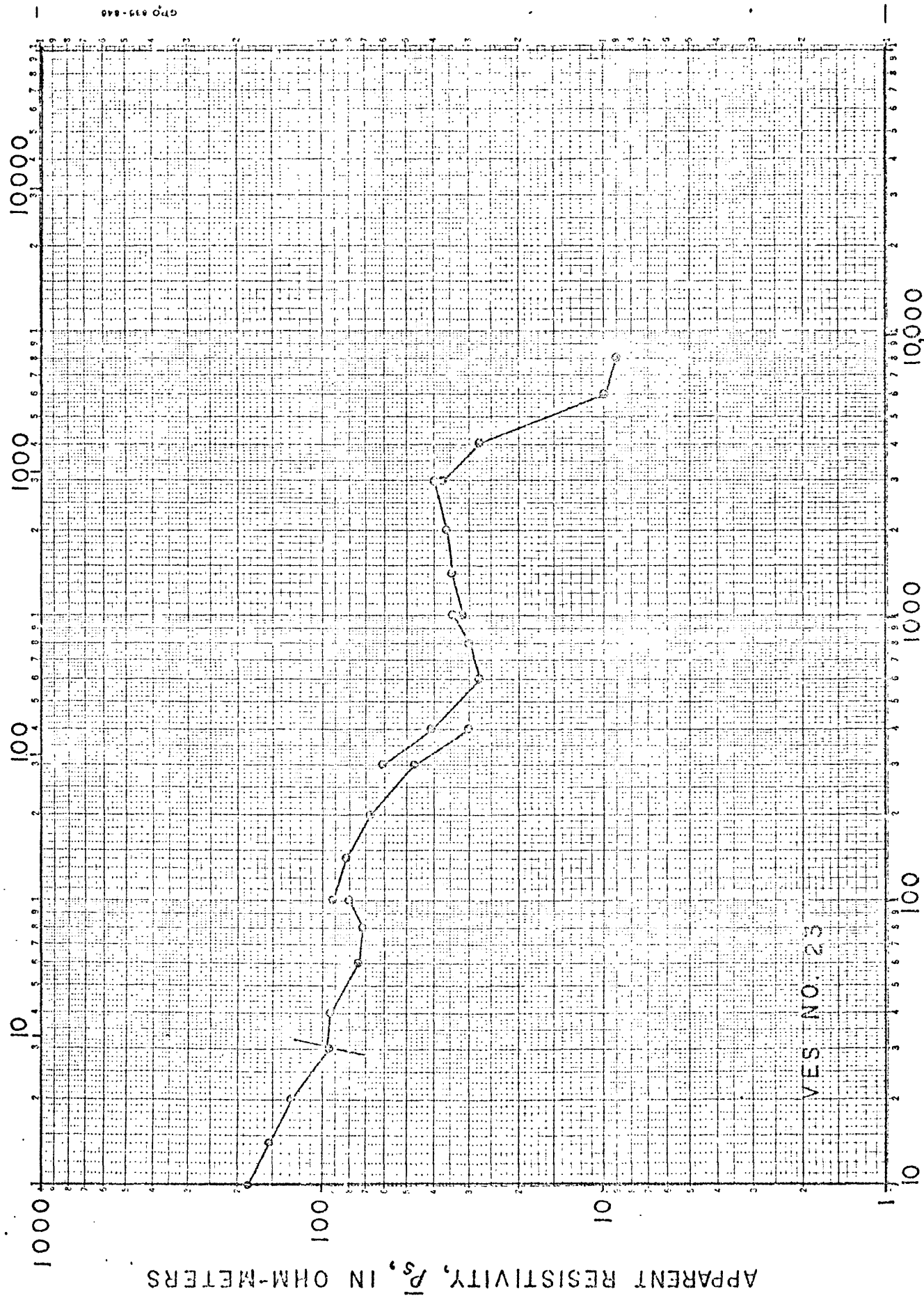ELECTRODE SPACING, AB/2, IN FEET

Figure 21.--Schlumberger curve VES 20

V.E.S. NO. 20

32

Figure 22.--Schlumberger curve VES 21

33
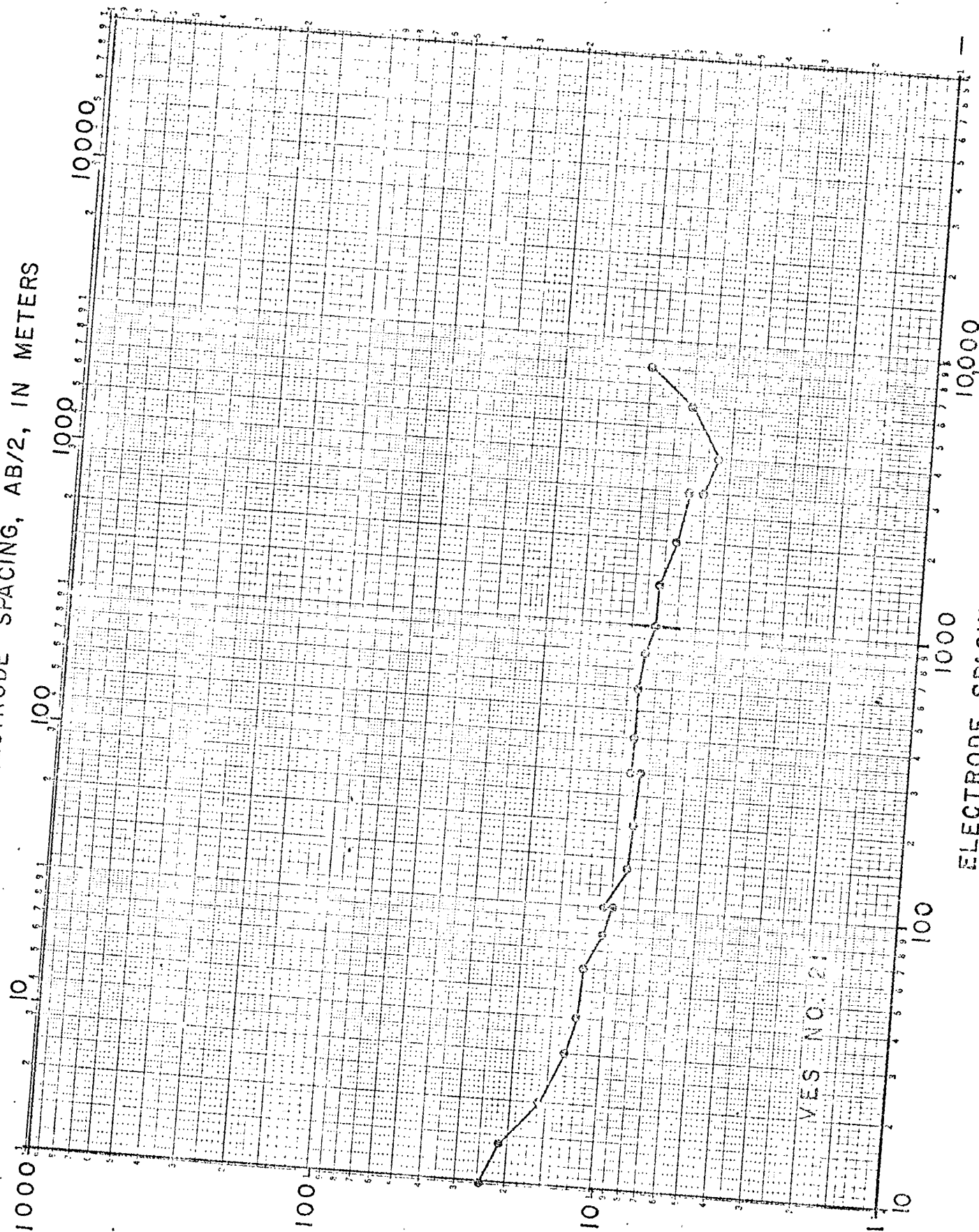
ELECTRODE SPACING, AB/2, IN METERS
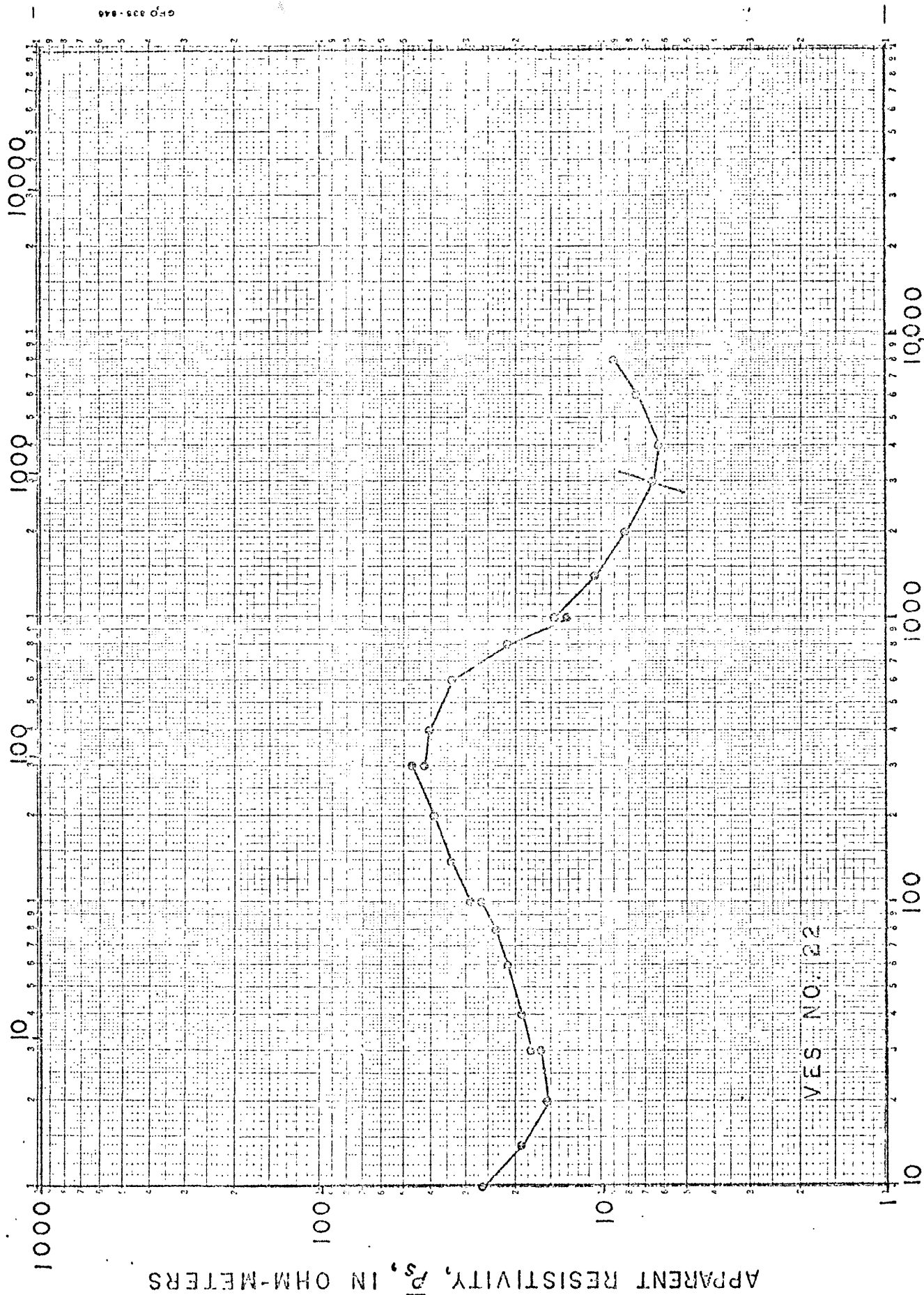
ELECTRODE SPACING, AB/2, IN FEET
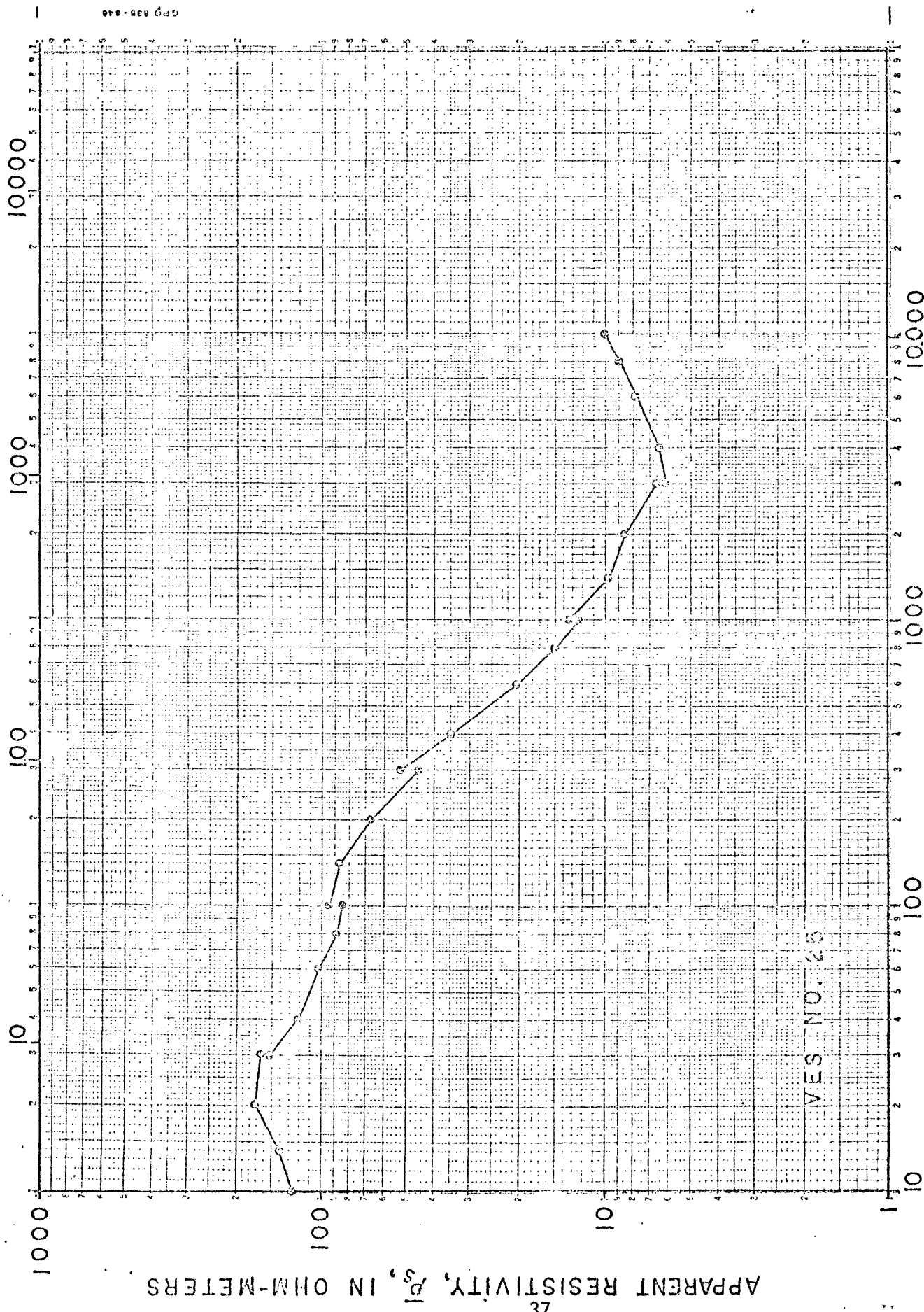
Figure 23.--Schlumberger curve VES 22

VES NO. 22

APPARENT RESISTIVITY, $\overline{\rho}_s$, IN OHM-METERS

34

ELECTRODE SPACING, AB/2, IN METERS

Figure 24.--Schlumberger curve VES 23

ELECTRODE SPACING, AB/2, IN FEET

VES. NO. 23

APPARENT RESISTIVITY, $\bar{P}_s$, IN OHM-METERS

GPO 813-840

35

ELECTRODE SPACING, AB/2, IN METERS

ELECTRODE SPACING, AB/2, IN FEET

APPARENT RESISTIVITY, $\bar{P}_s$, IN OHM-METERS

V.E.S. NO. 24
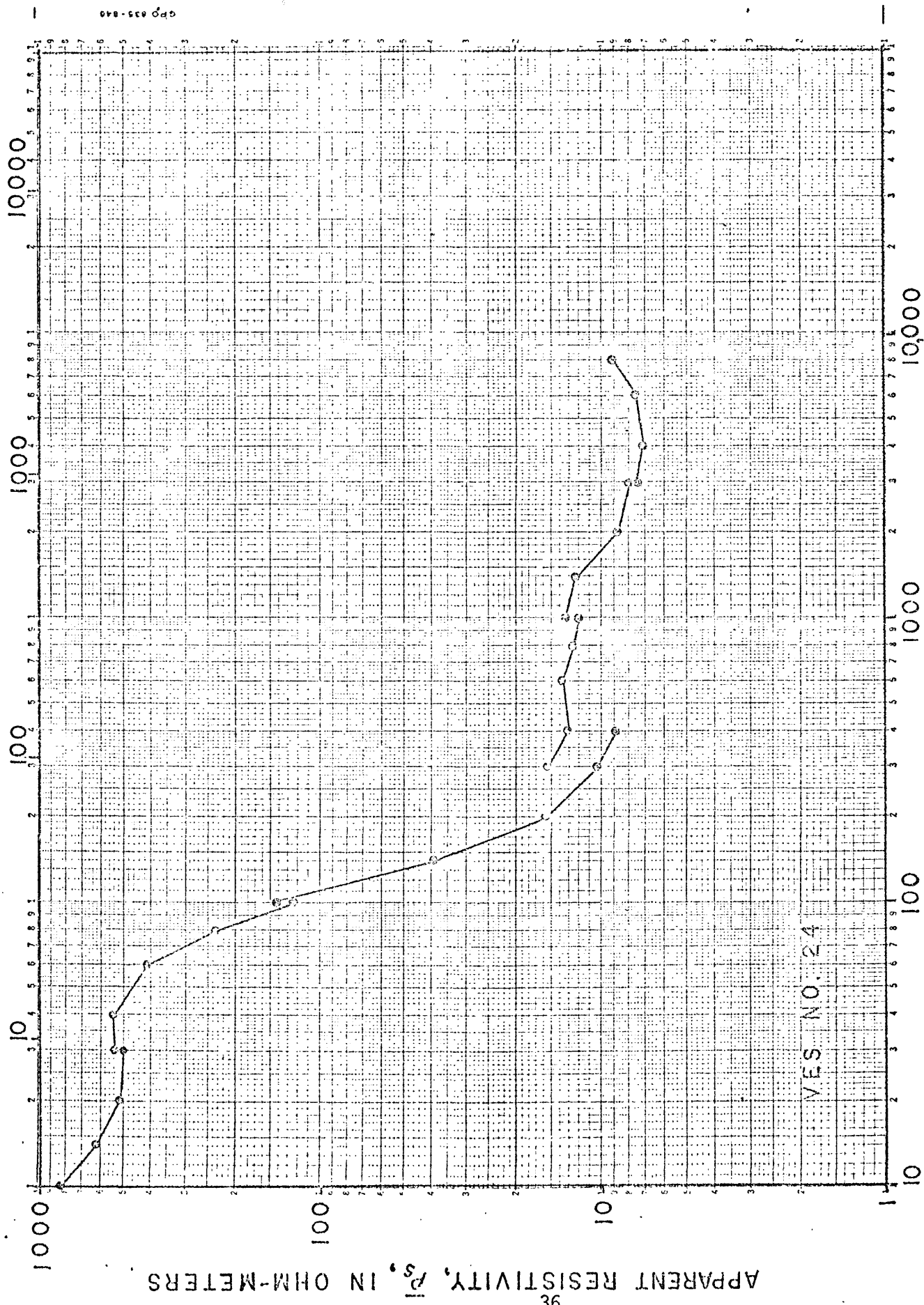
Figure 25.--Schlumberger curve VES 24

GPO 835-840

ELECTRODE SPACING, AB/2, IN METERS

APPARENT RESISTIVITY, $\underline{\rho}_s$, IN OHM-METERS
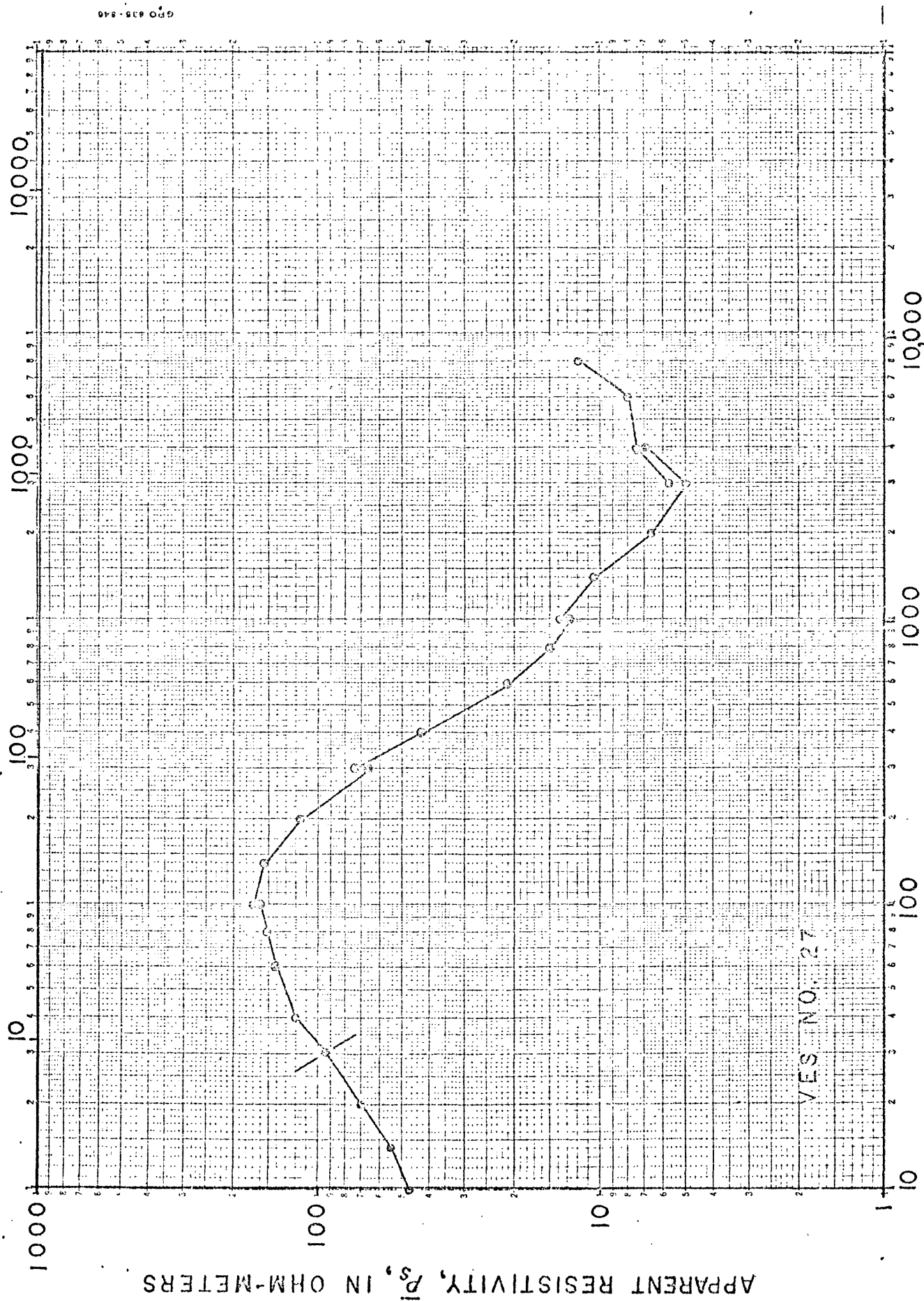
VES NO. 25

ELECTRODE SPACING, AB/2, IN FEET

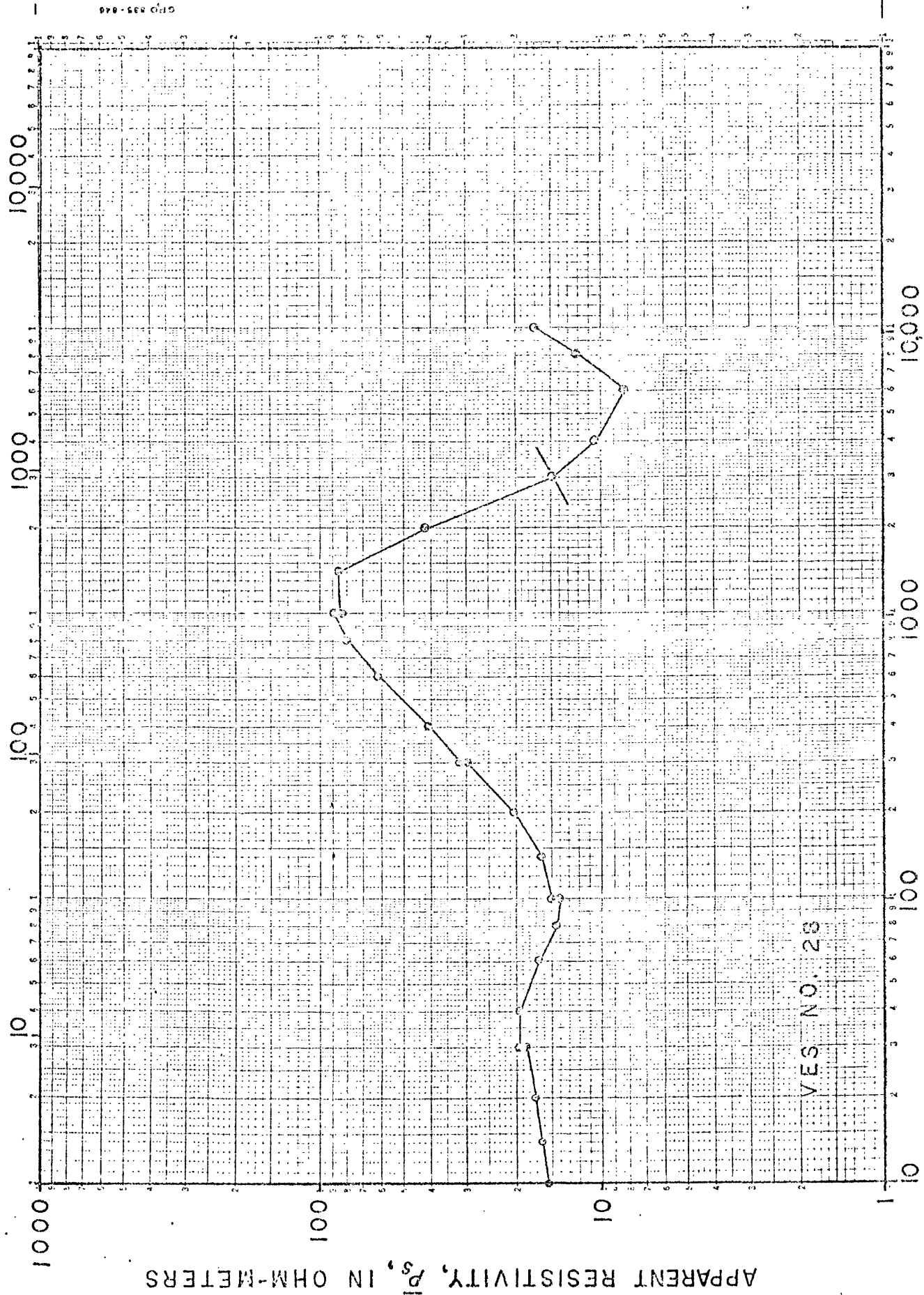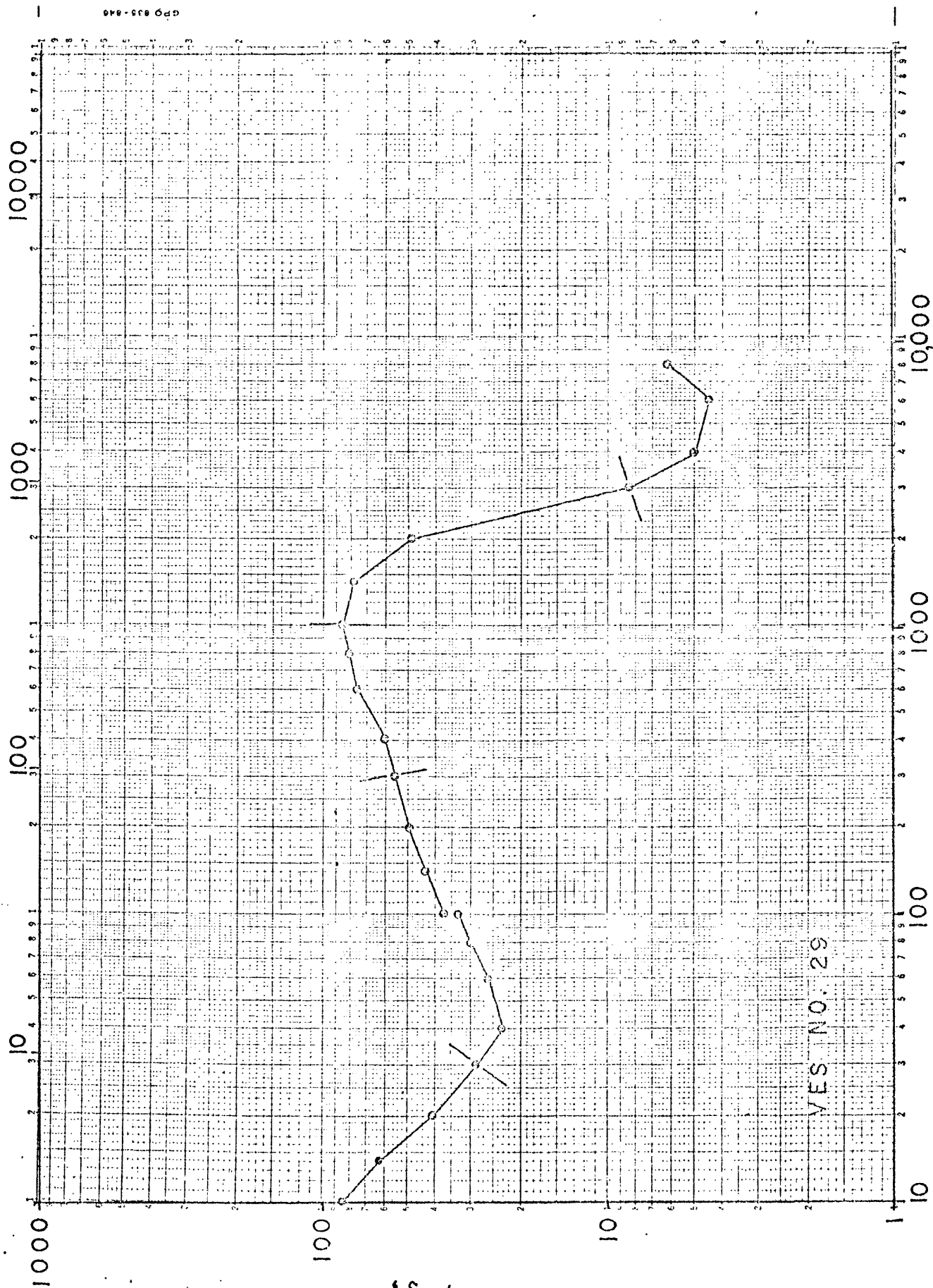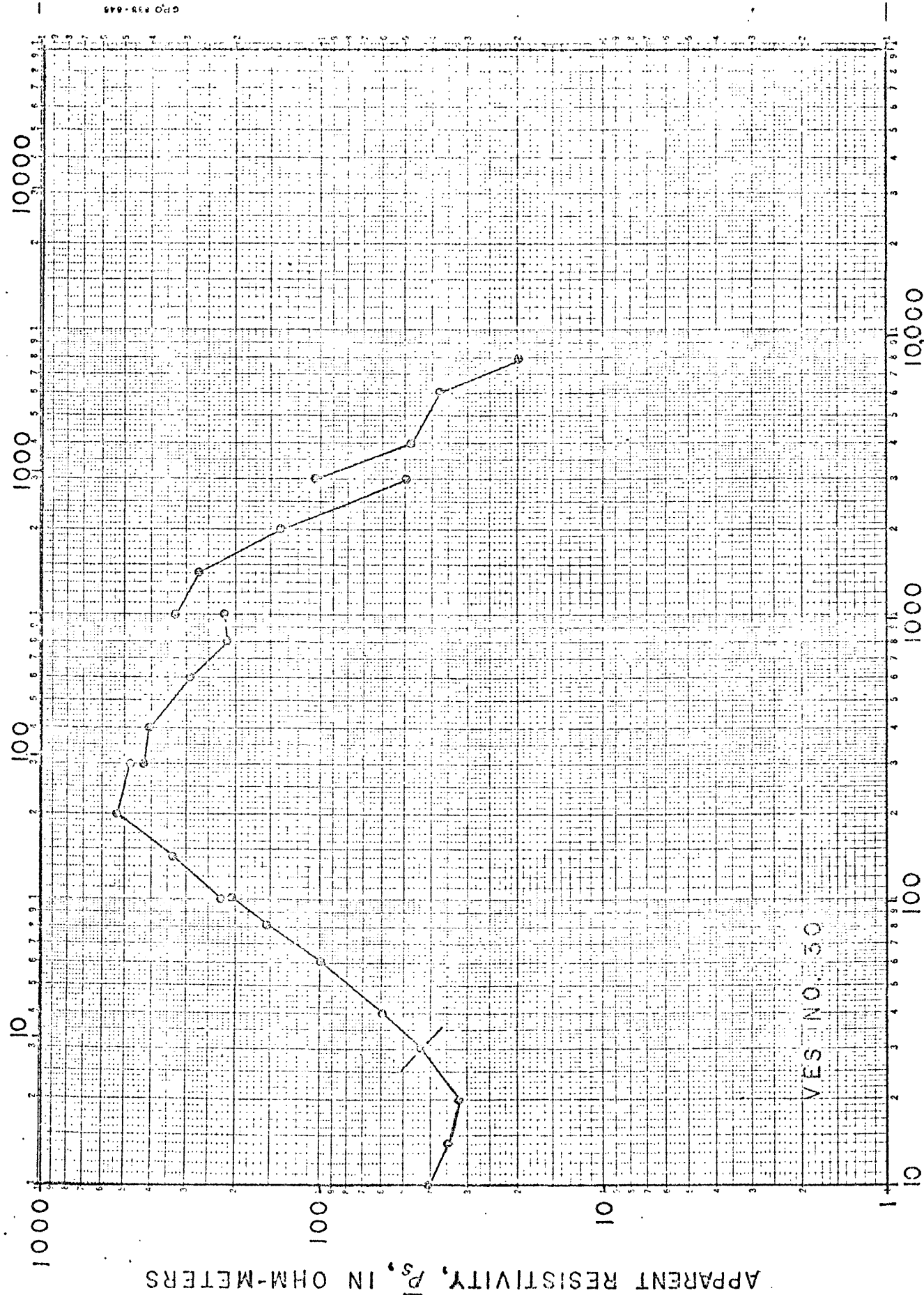Figure 26.--Schlumberger curve VES 25

37

ELECTRODE SPACING, AB/2, IN METERS
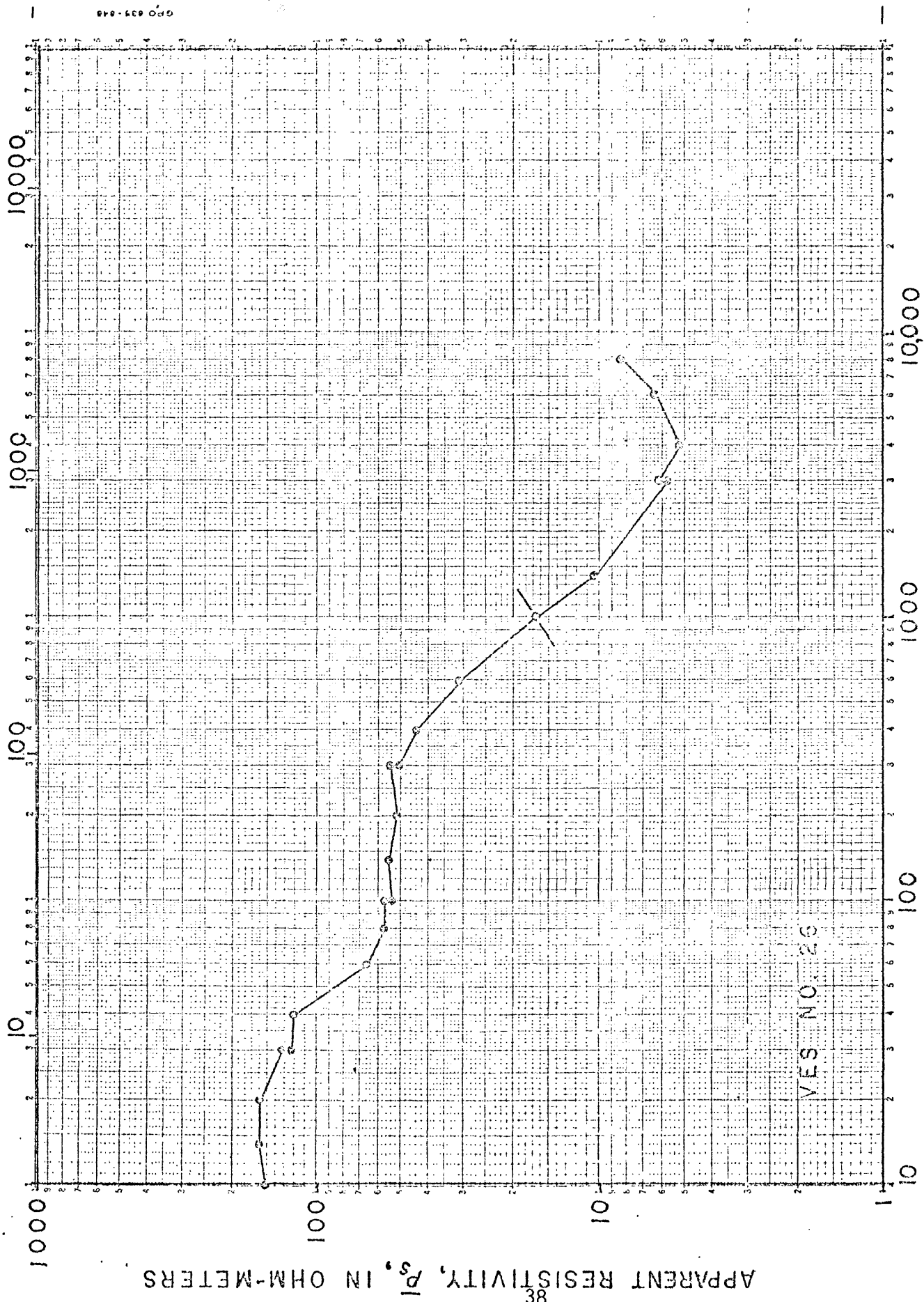
ELECTRODE SPACING, AB/2, IN FEET

Figure 27.--Schlumberger curve VES 26

APPARENT RESISTIVITY, $\bar{P}_s$, IN OHM-METERS

VES NO. 26

GPO 835-846

38

ELECTRODE SPACING, AB/2, IN METERS

ELECTRODE SPACING, AB/2, IN FEET

APPARENT RESISTIVITY, $\bar{P}_3$, IN OHM-METERS

VES NO. 27

Figure 28.--Schlumberger curve VES 27

ELECTRODE SPACING, AB/2, IN METERS

ELECTRODE SPACING, AB/2, IN FEET

APPARENT RESISTIVITY, $\overline{P}_s$, IN OHM-METERS

VES NO. 28

Figure 29.--Schlumberger curve VES 28

40

Figure 30.--Schlumberger curve VES 29

41

ELECTRODE SPACING, AB/2, IN METERS

Figure 31.--Schlumberger curve VES 30

ELECTRODE SPACING, AB/2, IN FEET

APPARENT RESISTIVITY, $\overline{P}_s$, IN OHM-METERS

VES NO. 30

42
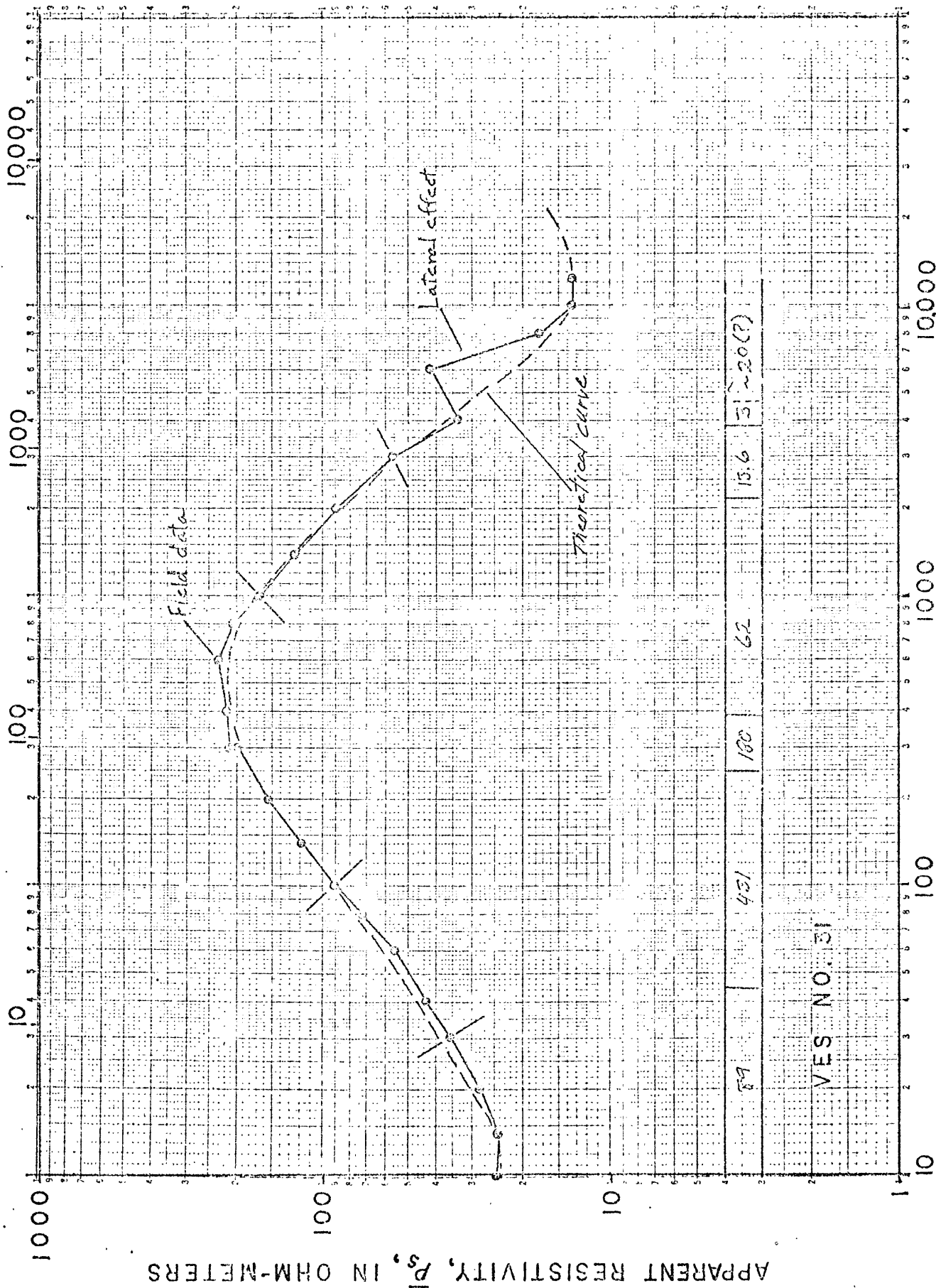
Figure 32.—VES 31 Schlumberger sounding curve showing layered resistivity model and theoretical apparent resistivity curve for the model.